

University of Windsor

Scholarship at UWindor

Electronic Theses and Dissertations

Theses, Dissertations, and Major Papers

2010

A Nano-Scale Chemical and Structural Characterization of Chinook Salmon (*Oncorhynchus tshawytscha*) Otoliths Using a FIB and HRTEM

Desirée E. Chevalier
University of Windsor

Follow this and additional works at: <https://scholar.uwindsor.ca/etd>

Recommended Citation

Chevalier, Desirée E., "A Nano-Scale Chemical and Structural Characterization of Chinook Salmon (*Oncorhynchus tshawytscha*) Otoliths Using a FIB and HRTEM" (2010). *Electronic Theses and Dissertations*. 8000.

<https://scholar.uwindsor.ca/etd/8000>

This online database contains the full-text of PhD dissertations and Masters' theses of University of Windsor students from 1954 forward. These documents are made available for personal study and research purposes only, in accordance with the Canadian Copyright Act and the Creative Commons license—CC BY-NC-ND (Attribution, Non-Commercial, No Derivative Works). Under this license, works must always be attributed to the copyright holder (original author), cannot be used for any commercial purposes, and may not be altered. Any other use would require the permission of the copyright holder. Students may inquire about withdrawing their dissertation and/or thesis from this database. For additional inquiries, please contact the repository administrator via email (scholarship@uwindsor.ca) or by telephone at 519-253-3000ext. 3208.

A Nano-Scale Chemical and Structural Characterization of Chinook Salmon
(*Oncorhynchus tshawytscha*) Otoliths Using a FIB and HRTEM

by

Desirée E. Chevalier

A Thesis
Submitted to the Faculty of Graduate Studies
Through the Great Lakes Institute for Environmental Research
In Partial Fulfillment of the Requirements for
The Degree of Master of Science at the
University of Windsor

Windsor, Ontario, Canada

2010

© 2010 Desiree Chevalier



Library and Archives
Canada

Published Heritage
Branch

395 Wellington Street
Ottawa ON K1A 0N4
Canada

Bibliothèque et
Archives Canada

Direction du
Patrimoine de l'édition

395, rue Wellington
Ottawa ON K1A 0N4
Canada

Your file *Votre référence*
ISBN: 978-0-494-70587-2
Our file *Notre référence*
ISBN: 978-0-494-70587-2

NOTICE:

The author has granted a non-exclusive license allowing Library and Archives Canada to reproduce, publish, archive, preserve, conserve, communicate to the public by telecommunication or on the Internet, loan, distribute and sell theses worldwide, for commercial or non-commercial purposes, in microform, paper, electronic and/or any other formats.

The author retains copyright ownership and moral rights in this thesis. Neither the thesis nor substantial extracts from it may be printed or otherwise reproduced without the author's permission.

AVIS:

L'auteur a accordé une licence non exclusive permettant à la Bibliothèque et Archives Canada de reproduire, publier, archiver, sauvegarder, conserver, transmettre au public par télécommunication ou par l'Internet, prêter, distribuer et vendre des thèses partout dans le monde, à des fins commerciales ou autres, sur support microforme, papier, électronique et/ou autres formats.

L'auteur conserve la propriété du droit d'auteur et des droits moraux qui protège cette thèse. Ni la thèse ni des extraits substantiels de celle-ci ne doivent être imprimés ou autrement reproduits sans son autorisation.

In compliance with the Canadian Privacy Act some supporting forms may have been removed from this thesis.

While these forms may be included in the document page count, their removal does not represent any loss of content from the thesis.

Conformément à la loi canadienne sur la protection de la vie privée, quelques formulaires secondaires ont été enlevés de cette thèse.

Bien que ces formulaires aient inclus dans la pagination, il n'y aura aucun contenu manquant.


Canada

ABSTRACT

We used a focused ion beam (FIB) to create thin sections from the post-hatch and core regions of Chinook salmon (*Oncorhynchus tshawytscha*) otoliths. The nano-scale chemistry and structure of these regions was characterized in thin section using scanning electron microscopy (SEM) in conjunction with cathodoluminescence (CL) and high resolution transmission electron microscopy (HRTEM). The results constrained the relative distribution of several elements; silicon-enriched nodules were found in the post-hatch otolith, and manganese, an element known to be enriched in the greater otolith core, was most concentrated at the center of primordia and at the primordia-core interfaces. Calcium was less abundant and carbon was observed in greater relative concentrations in the primordia relative to the surrounding core. HRTEM revealed a lack of crystallinity in the core relative to the post-hatch otolith. This is the first study to successfully thin-section an otolith using a FIB and characterize the thin section using HRTEM.

Declaration of Co-Authorship / Previous Publication

I. Co-Authorship Declaration

I hereby declare that this thesis incorporates material that is result of joint research, as follows: This thesis incorporates the outcome of a joint research undertaken in collaboration with Dr. Joel Gagnon, Dr. Todd Simpson, and Dr. Christopher Weisener. The collaboration is covered in Chapter 2 of the thesis. In all cases, the key ideas, primary contributions, experimental designs, data analysis and interpretation, were performed by the author, and the contribution of co-authors was primarily through the provision of assistance with the development of methodology and assistance with instrumentation.

I am aware of the University of Windsor Senate Policy on Authorship and I certify that I have properly acknowledged the contribution of other researchers to my thesis, and have obtained written permission from each of the co-author(s) to include the above material(s) in my thesis.

I certify that, with the above qualification, this thesis, and the research to which it refers, is the product of my own work.

II. Declaration of Previous Publication

This thesis includes one original paper that has been previously submitted for publication in peer reviewed journals, as follows:

Thesis Chapter	Publication title/full citation	Publication status*
Chapter 2	The nano-scale chemical and structural characterization of Chinook salmon (<i>Oncorhynchus tshawytscha</i>) otolith cores using a FIB and HRTEM	<i>Submitted to Environmental Science and Technology</i>

I certify that I have obtained a written permission from the copyright owner(s) to include the above published material(s) in my thesis. I certify that the above material describes work completed during my registration as graduate student at the University of Windsor.

I declare that, to the best of my knowledge, my thesis does not infringe upon anyone's copyright nor violate any proprietary rights and that any ideas, techniques, quotations, or any other material from the work of other people included in my thesis, published or otherwise, are fully acknowledged in accordance with the standard referencing practices. Furthermore, to the extent that I have included copyrighted material that surpasses the bounds of fair dealing within the meaning of the Canada Copyright Act, I certify that I have obtained a written permission from the copyright owner(s) to include such material(s) in my thesis.

I declare that this is a true copy of my thesis, including any final revisions, as approved by my thesis committee and the Graduate Studies office, and that this thesis has not been submitted for a higher degree to any other University or Institution.

ACKNOWLEDGEMENTS

I would like to dedicate this work to my father, whose love of nature and learning continue to inspire me even in his absence.

First, I would like to acknowledge Dr. Joel Gagnon and Dr. Christopher Weisener for their continual support and guidance throughout this project. With their help, I was able to design and apply a new methodology that encompassed several disciplines and was both challenging and endlessly fascinating. I would also like to thank my committee members, Dr. Brian Fryer, Dr. Iain Samson and Dr. Phil Graniero, for their interest and support of this project. In addition, I would like to thank Dr. Todd Simpson from the University of Western Ontario for his interest in our project and all his assistance developing the FIB methodology. Support for TEM analysis was graciously provided by Dr. Carmen Andrei, at McMaster University. Assistance with SEM analysis and imaging was provided by Ms. Sharon Lackie, whose expertise and dedication have been greatly appreciated. I would also like to express my sincere thanks to Ms. Christina Smeaton for her assistance with data analysis and support throughout the writing process. Assistance with data analysis and sample preparation was kindly provided by Ms. Melissa Price, Dr. Sonia Melancon, Dr. Zhe Song and Dr. Derek Hogan. A special thanks to Dr. Brian Fryer, Dr. Yolanda Morbey at the University of Western Ontario and Dr. Daniel Heath and Yellow Island Aquaculture for providing otolith samples. I would also like to thank Mrs. Mary Lou Scratch,

Mrs. Connie Iaquina and Dr. Aaron Fisk for all their help during my time at GLIER. Lastly, I would like to thank my family and friends for all their love and encouragement through this process.

TABLE OF CONTENTS

ABSTRACT.....	iii
DECLARATION OF CO-AUTHORSHIP/PREVIOUS PUBLICATION.....	iv
ACKNOWLEDGEMENTS.....	v
LIST OF TABLES.....	viii
LIST OF FIGURES.....	ix
 CHAPTER 1: Introduction.....	 1
1.1 THE PROBLEM.....	2
1.2 BACKGROUND.....	3
1.2-1 The function and composition of otoliths.....	3
1.2-2 The teleost otolith: Use in elemental “fingerprinting”.....	4
1.2-3 The otolith core: Microchemistry and microstructure.....	5
1.2-4 Resolving scale-based limitations	8
1.3 OBJECTIVES.....	12
1.4 LITERATURE CITED.....	14
 CHAPTER 2: A nano-scale chemical and structural characterization of Chinook salmon (<i>Oncorhynchus tshawytscha</i>) otolith core using a FIB and HRTEM.....	 20
2.1 INTRODUCTION.....	21
2.2 MATERIALS AND METHODS.....	23
2.2-1 Extraction and sectioning of otoliths.....	24
2.2-2 Application of reference marks.....	24
2.2-3 SEM-CL and SEM-EDS analysis.....	25
2.2-4 FIB/SEM analysis.....	26
2.2-5 HRTEM analysis.....	29
2.3 RESULTS.....	29
2.3-1 Identification and preliminary micro-scale chemical characterization of core region using SEM-CL and SEM- EDS.....	29
2.3-2 Thin sectioning and preliminary micro-scale chemical characterization using FIB/SEM.....	31
2.3-3 Nano-scale characterization of otolith chemistry and structure using HRTEM.....	33
2.4 DISCUSSION.....	36
2.5 LITERATURE CITED.....	38
 CHAPTER 3: Summary, suggestions for future work and conclusions.....	 42
3.1 SUMMARY.....	43
3.2 SUGGESTIONS FOR FUTURE WORK.....	44
3.3 CONCLUSIONS.....	45
3.4 LITERATURE CITED.....	48
 VITA AUCTORIS.....	 64

LIST OF TABLES

Table 1	EDS spectra collected from thin section milled from the post-hatch otolith (6 locations)	49
Table 2	D-spacing values collected from a thin section milled from the post-hatch otolith (8 locations)	50
Table 3	D-spacing values collected from a thin section milled of the otolith core region (4 locations)	51
Table 4	EDS spectra collected from thin section milled of the otolith core region (8 locations)	52

LIST OF FIGURES

Figure 1	SEM-SE image of sample surface with FIB-milled grid surrounding the otolith core.	53
Figure 2	A) SEM-SE image of two trenches milled using a FIB on either side of a created thin section prior to lift-out. B) Thin-section lift-out using a pair of tines cut in the tip of a TEM grid-sized Mo foil.	54
Figure 3	A) SEM-BSE image of the core region after collection of SEM-EDS maps noting some electron beam damage that was incurred. B) SEM-BSE image of core region prior to SEM-EDS mapping highlighting a porous region thought to be the result of loss of organic content during storage.	55
Figure 4	A) SEM-BSE image of an otolith after polishing showing the distribution of manganese (cps) across an SEM-EDS line scan region through the otolith core and several primordia. B) SEM-CL image of the region shown in Figure 4A showing the luminescence of first few daily increments and three luminescent primordia.	56
Figure 5	SEM-CL image of the core region of a polished otolith. Daily increments are visible occurring in concentric bands surrounding a luminescent central core region.	57
Figure 6	A) SEM-BSE image of otolith core region. B) SEM-EDS maps of C, O, Ca and Mn collected from sample surface shown in Figure 6A.	58
Figure 7	A) TEM-HAADF image of thin section milled from a region of the post-hatch otolith highlighting round, silicon-enriched nodules in the sample. B) TEM-HAADF image of nodules and locations where EDS spectra were collected.	59
Figure 8	FFT of locations denoted in Table 2 with d-spacings inset.	60

Figure 9	A) TEM-BF image of thin section milled to include the otolith core showing multiple primordia throughout the region with numbered regions indicating locations where high resolution images were collected. B) TEM-BF image of the interface between a primordium and the rest of the otolith core with FFT images and d-spacings calculated from images of the area.	61
Figure 10	FFT of locations denoted in Table 3.	62
Figure 11	A) TEM-HAADF image of a single primordium in the thin section milled to include the otolith core region. Numbered boxed regions denote areas for EDS spectral analysis. B) STEM element maps of C, Ca, O and Mn collected from the primordium shown in (A).	63

CHAPTER 1

Introduction

1.1 THE PROBLEM

The otolith has quickly become regarded as one of the most important tools in modern fisheries research. Providing a record of age and environmental exposure throughout life in teleost fish, this information can reveal life history events and be used to discern stock populations. The otolith also possesses information regarding the embryonic life of fish (i.e., the otolith core). Formed in some species just a few days after fertilization, the otolith core is the pre-hatch portion of the otolith and contains valuable chemical information because it incorporates elements from both the natal habitat site as well as maternal associations via the yolk sac. Understanding core chemistry in particular is important for conservation management and provides insight into the mechanisms of early otolith formation.

Although high resolution microscopy methods, such as transmission electron microscopy (TEM), are commonly used for nano-scale chemical and structural characterization in minerals, these high resolution methods require the creation of thin sections only a few hundred nanometers thickness. Biominerals, such as otoliths, do not possess the same structural integrity as most minerals due to the presence of organics in the structure, which makes the creation of such thin sections difficult or impossible. Physical methods of creating thin sections cannot produce sections of appropriate thickness due to fracturing during the toming process. The only prior alternative to the creation of a physically-milled thin section was to follow a complex methodology of

sample preparation that often involved the loss of mineral or biological content from the otolith through grinding or demineralization of the sample and subsequent chemical treatment.

The use of a focused ion beam (FIB) for production of thin sections was originally developed in materials science but has recently become popular in the creation of thin sections in biominerals as well. Despite the presence of organic content in these biominerals, the use of a FIB has enabled users to mill thin sections without damaging the sample and without complex sample preparation. Additionally, this method does not result the demineralization of the sample or loss of organic content. A FIB is also used commonly in conjunction with scanning electron microscopy (SEM), which uses an electron beam to provide images immediately before or after thin section milling using a FIB.

The goal of this study is to develop a method for creating thin sections from both the core and the post-hatch regions of Chinook salmon (*Oncorhynchus tshawytscha*) otoliths using a FIB in conjunction with SEM and to provide the first nano-scale chemical and structural characterization of FIB-milled thin sections using high resolution transmission electron microscopy (HRTEM).

1.2 BACKGROUND

1.2-1 The function and composition of otoliths

Otoconia are biominerals found in the inner ear of vertebrates and are necessary for hearing and balance (HUGHES et al., 2004). Composed largely (~ 97%) of calcium carbonate (CaCO_3) in an organic matrix of glycoproteins and proteoglycans (~ 0.2 to 10%), the otoconia form during the embryonic stage and are maintained throughout life (BORELLI et al., 2003; DEGENS et al., 1969; HUGHES et al., 2004; MURAYAMA et al., 2000; MURAYAMA et al., 2002). In teleost (bony) fish, the otoconia are termed otoliths. Although otoliths have a function and composition similar to the otoconia of other vertebrates, they have a different structure and grow throughout life by forming daily layers accreted from the endolymph fluid of the inner ear (BORELLI et al., 2003; HUGHES et al., 2004).

1.2-2 The teleost otolith: Use in elemental “fingerprinting”

The chemistry of the endolymph fluid has been shown to be influenced by the ambient environment. As water passes through the gills of the fish to provide oxygen to the blood, trace elements, along with calcium, carbonate and bicarbonate ions and dissolved inorganic carbon are incorporated into the blood and then into the endolymph fluid (CAMPANA, 1999). As a result, an individual otolith will possess a trace element “fingerprint” (< 1% of whole otolith) that has been considered reflective of the life history of the individual

(CAMPANA et al., 2000). The presence of this trace element signature, along with the fact that the inorganic components of teleost otoliths (unlike human otoconia) are thought not to be subject to re-absorption after incorporation, makes otoliths a valuable and commonly-used tool in fisheries science (CAMPANA, 1999).

Otolith micro-chemical assays using LA-ICP-MS (laser ablation inductively coupled plasma mass spectrometry) have applications for stock delineation of fish as well as for the assessment of population migration, structure and mixing, and life-history strategies (CAMPANA, 1999; THRESHER, 1999). Additionally, the microchemistry of the otolith core, which is the portion of the otolith that forms during the embryonic stage, has become the focus of several recent studies because its chemistry is considered reflective of natal habitats and maternal signatures in individuals (BROPHY et al., 2004; CAMPANA et al., 2000; MILLER and KENT, 2009; SECOR et al., 2001; VOLK et al., 2000; WARNER et al., 2005).

1.2-3 The otolith core: microchemistry and microstructure

Typically less than 20 μm in diameter, the core houses the primordium, which is the site of initial nucleation in the otolith (0.5 to 1 μm diameter) (KALISH et al., 1995). In some fish species, such as salmonids, there are multiple primordia (which may be separate or fused), whereas in other species, only one is present (SOKOLOWSKI, 1986). Chemical assays of the otolith core can be challenging due to its small size and while LA-ICP-MS

has a resolution capable of differentiating the composition of the otolith core from the remainder of the otolith, it cannot provide a nano-scale chemical characterization of the core.

Studies by several authors have provided evidence that the core possesses a greater concentration of organic content, an amorphous structure, as well as a significantly higher concentration of the element manganese (Mn) compared to the post-hatch otolith (BEIER and ANKEN, 2006; BROPHY et al., 2004; CARLSTROM, 1963; DEGENS et al., 1969; FREEMAN et al., 2008; JOLIVET et al., 2008; MELANCON et al., 2008; MURAYAMA et al., 2004; POUGET et al., 2009; RUTTENBERG et al., 2005; SOKOLOWSKI, 1986; ZHANG and RUNHAM, 1992). The determinations of element concentrations using LA-ICP-MS typically assume that the otolith core comprises exclusively inorganic material (i.e., 100% aragonite). Therefore, it is necessary to fully understand otolith core composition to ensure: 1. the accuracy of elemental data obtained using LA-ICP-MS and 2. the validity of interpretations regarding the early life history of fish that are inferred from these data.

There are several reasons why more organic content might be observed in the otolith core compared with the region of the otolith formed later after hatch. Degens et al., (1969), presented the first research on otolith proteins. Their isolation of a 150,000 molecular weight (MW) protein, which they termed otolin, led them to the conclusion that proteins found in the organic matrix of the otolith (which comprises about ~ 0.2 to 10% of the otolith) were necessary for the nucleation of the otolith primordia (DEGENS et

al., 1969). They presented a theory that protein was associated with mineralization because it contained a large proportion of oxygen-rich amino acids that were bound to calcium ions (DEGENS et al., 1969). The subsequent nucleation and crystal growth produced the aragonite polymorph of calcium carbonate (DEGENS et al., 1969). Later studies would provide evidence to support the theory presented by Degens et al. (1969) by showing that proteins (and their associated enzymes) were necessary for normal formation of mollusk shells and otoliths (BELCHER et al., 1996; MURAYAMA et al., 2004; SOLLNER et al., 2003). The enzyme carbonic anhydrase (CAH), which provides carbonate for CaCO_3 formation, is an example of such a protein product (BEIER and ANKEN, 2006).

While higher organic concentrations may be the cause of the lack of crystallinity observed in the otolith core, some research has suggested the early core is composed of a mineraloid called amorphous calcium carbonate (ACC) (FREEMAN et al., 2008; LOWENSTAM, 1981; NEUMANN and EPPLE, 2007; POUGET et al., 2009; ROSAUER and REDMOND, 1985; SOKOLOWSKI, 1986). It is thought that ACC nanoparticles nucleate as a precursor phase in carbonates before undergoing a rearrangement event to crystalline CaCO_3 (FREEMAN et al., 2008; LOWENSTAM, 1981; NEUMANN and EPPLE, 2007; POUGET et al., 2009; ROSAUER and REDMOND, 1985; SOKOLOWSKI, 1986). These studies also suggest that the ACC that composes the early otolith is reduced to only trace quantities by adulthood (LOWENSTAM, 1981; NEUMANN and EPPLE, 2007; SOKOLOWSKI, 1986).

The evidence for abundant organics and an amorphous structure in the core is not found in the post-hatch otolith. In particular, the identification of Mn peaks in the cores of otoliths illustrates the compositional differences between the otolith core and the post-hatch otolith. Ruttenberg et al. (2005) found using LA-ICP-MS that otolith cores analyzed across six different species of fish were shown consistently to have elevated concentrations of Mn in comparison with the region adjacent to the otolith core region. The core was considered to have a Mn spike if the Mn concentration was at least three times greater than the previous site of ablation (RUTTENBERG et al., 2005). The presence of an increased concentration of Mn in the otolith core implies a relationship between the early development of fish and Mn. Studies in the otoconia of other vertebrates, including rats, birds and reptiles, have shown Mn deficiencies during development to cause otolith defects and subsequent detrimental effects on animal behavior and survival (ERWAY et al., 1971; ERWAY et al., 1986; HORI and IWASAKI, 1976).

Melancon et al. (2008) also noted in their study of otolith micro-chemistry using LA-ICP-MS that the calculated concentration of Mn at the centre of the core (the primordia) might be underestimated due to technological limitations of LA-ICP-MS (a volume of material larger than the otolith primordia itself was sampled). While LA-ICP-MS is useful for differentiating the core from the post-hatch otolith, it cannot be used to address questions of nano-scale chemistry and structure that can provide

further insights into otolith development, natal habitat, and the characterization of maternal associations.

1.2-4 Resolving scale-based limitations

The development of a high-resolution methodology that limits or does not require the loss of any organic or inorganic components is desirable for the characterization of the nano-scale structure and chemistry of the otolith core.

While wavelength-dispersive electron microprobe (WD-EM) and energy-dispersive electron microprobe (ED-EM) have both been used for targeted elemental analysis in fish otoliths, only LA-ICP-MS and nuclear microscopy using proton-induced x-ray emission (μ PIXE) methods have been found to provide the resolution necessary for the analysis of trace elements within the otolith structure (with the exception of Sr, which could also be detected and analyzed using WD-EM) (CAMPANA et al., 1997). LA-ICP-MS spot size is too large for nano-scale chemical analysis and results in permanent loss of the sample, while the results of μ PIXE in otoliths can be difficult to interpret due to interference from sodium (Na) (LIMBURG et al., 2003; LIMBURG et al., 2007). Electron microprobes, while able to provide micro-scale maps, can only detect elements with a concentration in the parts per thousand range, which is significantly more concentrated than the levels that most trace elements occur at in otoliths (LIMBURG et al., 2007).

Scale-based limitations have been identified in the analysis of other biominerals as well (i.e., teeth and shells). In these studies, HRTEM and synchrotron x-ray fluorescence (XRF) methods have been used to provide improved spatial resolution of the chemistry and structure present without damage to the sample (KUDO et al., 2010; LIMBURG et al., 2007; NALLA et al., 2005; SAUNDERS et al., 2009; TEMPLETON and KNOWLES, 2009; WIRTH, 2009). The challenge in pursuing these methods of analyses is in the sample preparation. Resolving the structure of the sample requires the sample to be in a thin section (ideally ~ 150 nm thick) to allow the penetration of either an electron beam (HRTEM) or x-rays (synchrotron XRF) (TEMPLETON and KNOWLES, 2009). The production of a thin section ~ 150 nm thick cannot easily be achieved through physical sectioning methods (toming), likely due to structural instability in the sample as a result of the organic content present.

A possible solution to this dilemma is the use of a FIB. This approach uses a beam of gallium (Ga) ions approximately 2 to 5 nm in diameter that interacts with the sample surface causing a sputtering of atoms, which allows for the selective milling of thin sections (STOKES et al., 2006; WIRTH, 2009). Additionally, most FIBs are also equipped with an SEM that allows real-time imaging of the sample through the interaction of a beam of electrons with the sample surface, which causes ions and secondary electrons to be emitted and used to form an image (STOKES et al., 2006). A FIB has already been used successfully to create thin sections from several biominerals including shells, teeth and bones (KUDO et al., 2010; NALLA et al., 2005; SAUNDERS et

al., 2009), although it has not yet been used in the creation of thin-sections from otoliths.

In principle, the production of a thin section from an otolith using a FIB does not present a challenge. The challenge, however, lies in developing a methodology to create a thin section from a specific site of interest, in this case, the otolith core. A method of identifying the approximate location of the core compatible with the SEM imaging used in real time while FIB milling the thin section is required. Otolith growth structures (daily growth rings and primordia) are not easily imaged using SEM because the trace element variation is often below the detection limit. SEM used in conjunction with a cathodoluminescence (CL) detector, however, could be used to successfully image growth textures in otoliths. CL uses a photon beam to excite the electrons at the sample surface causing the emission of electromagnetic radiation from the sample (luminescence) within the visible range (HALDEN et al., 2004). Halden et al. (2004) demonstrated using CL and PIXE, that otolith regions with the highest Mn concentrations had the brightest luminescence, making the otolith core one of the most visible growth features using CL based on the Mn-enrichment in the core relative to the post-hatch otolith (BROPHY et al., 2004; HALDEN et al., 2004; MELANCON et al., 2008; RUTTENBERG et al., 2005). SEM-CL also possesses an advantage over traditional CL because it can be combined with energy dispersive x-ray spectroscopy (EDS) on the SEM, producing $\mu\text{g/g}$ range chemical maps of an area after CL imaging (LANDTWING and PETTKE, 2005). SEM-CL has been

favoured for the characterization of growth textures in minerals such as quartz (LANDTWING and PETTKE, 2005), and was also used to discriminate between CaCO_3 polymorphs in otoliths (BEAREZ et al., 2005). An inherent problem with imaging otolith cores using SEM-CL is the low success rate associated with the exposure of the otolith core via manual polishing with lapping film. SEM-CL is a surface technique and if the otolith core is not exposed, luminescence may not be observed. This could potentially necessitate the preparation of a relatively large number of samples for SEM-CL analysis.

Using SEM-CL to locate the otolith core and successive milling using a FIB constitutes a new methodology for the production of thin sections suitable for high resolution microscopy that potentially does not involve any loss of organic or inorganic content in the otolith. HRTEM is a relatively accessible technology that can be used to perform a nano-scale chemical and structural characterization of the FIB-milled otolith thin section. High-resolution EDS can be conducted using HRTEM to provide chemical information about the sample and fast Fourier transform (FFT) of the images can be used to characterize crystalline phases present (BENDERSKY and GAYLE, 2001). HRTEM is not a technique that has been used in otoliths in recent years for the purpose of characterizing chemistry possibly due to the extensive sample preparation that would be required to ready the sample for imaging. Without a method of creating a thin-section through some means of physical milling, the only way to gain insight into the nano-structures and chemistry of the sample would be through the grinding and subsequent chemical treatment of the

otolith-derived supernatant (LI et al., 2009). When contrasted with the method of FIB sectioning for HRTEM analysis, which has been conducted in geomaterials and several biominerals, there is a wealth of structural and mineralogical data to be gathered without loss of organic or inorganic components and complex sample preparation (KUDO et al., 2010; NALLA et al., 2005; SAUNDERS et al., 2009; WIRTH, 2009).

1.3 OBJECTIVES

The objectives of this study are:

- 1) The development of a methodology that can be used to;
 - i) Identify the otolith core
 - ii) Provide a preliminary micro-scale chemical characterization
 - iii) Produce a thin section from the otolith using a FIB
- 2) Conduct nano-scale chemical and structural characterization of otoliths using thin sections created following the methodology outlined in (1) in conjunction with HRTEM.
- 3) Interpret this data in the context of the current understanding of otolith formation and structure.

This information may be useful for those seeking higher-resolution alternatives to typical LA-ICP-MS analyses in otolith trace element assays. For example, Chinook salmon are an anadromous sport fish and conservation

and management specialists often rely on core microchemistry in the identification of natal habitats and life history characteristics in juveniles to make management decisions (KALISH, 1999; VOLK et al., 2000; WARNER et al., 2005; ZHANG and BEAMISH, 2000). Additionally, if the otolith core can be successfully thin-sectioned, the structural and chemical information obtained will provide further data on the development of the early otolith which may facilitate an improved understanding of early otolith formation and biomineralization.

1.4 LITERATURE CITED

- Bearez P., Carlier G., Lorand J. P., and Parodi G. C. (2005) Destructive and non-destructive microanalysis of biocarbonates applied to anomalous otoliths of archaeological and modern *sciaenids* (Teleostei) from Peru and Chile. *Comptes Rendus Biologies* **328**(3), 243-252.
- Bendersky L. A. and Gayle F. W. (2001) Electron diffraction using transmission electron microscopy. *Journal of Research of the National Institute of Standards and Technology* **106**(6), 997-1012.
- Beier M. and Anken R. (2006) On the role of carbonic anhydrase in the early phase of fish otolith mineralization. In *Space Life Sciences*, Vol. 38 (ed. L. L. Bruce and C. Dournon), pp. 1119-1122.
- Belcher A. M., Wu X. H., Christensen R. J., Hansma P. K., Stucky G. D., and Morse D. E. (1996) Control of crystal phase switching and orientation by soluble mollusc-shell proteins. *Nature* **381**(6577), 56-58.
- Borelli G., Mayer-Gostan N., Merle P. L., De Pontual H., Boeuf G., Allemand D., and Payan P. (2003) Composition of biomineral organic matrices with special emphasis on turbot (*Psetta maxima*) otolith and endolymph. *Calcified Tissue International* **72**(6), 717-725.
- Brophy D., Jeffries T. E., and Danilowicz B. S. (2004) Elevated manganese concentrations at the cores of clupeid otoliths: possible environmental, physiological, or structural origins. *Marine Biology* **144**(4), 779-786.
- Campana S. E. (1999) Chemistry and composition of fish otoliths: pathways, mechanisms and applications. *Marine Ecology-Progress Series* **188**, 263-297.
- Campana S. E., Chouinard G. A., Hanson J. M., Frechet A., and Bratney J. (2000) Otolith elemental fingerprints as biological tracers of fish stocks. *Fisheries Research* **46**(1-3), 343-357.
- Campana S. E., Thorrold S. R., Jones C. M., Gunther D., Tubrett M., Longerich H., Jackson S., Halden N. M., Kalish J. M., Piccoli P., dePontual H., Troadec H., Panfili J., Secor D. H., Severin K. P., Sie S. H., Thresher R., Teesdale W. J., and Campbell J. L. (1997) Comparison of accuracy, precision, and sensitivity in elemental assays of fish otoliths using the electron microprobe, proton-induced X-ray emission, and laser ablation inductively coupled plasma mass spectrometry. *Canadian Journal of Fisheries and Aquatic Sciences* **54**(9), 2068-2079.

- Carlstrom D. (1963) A Crystallographic Study of Vertebrate Otoliths. *Biological Bulletin* **125**(3), 441-463.
- Degens E. T., Deuser W. G., and Haedrich R. L. (1969) Molecular Structure and Composition of Fish Otoliths. *Marine Biology* **2**(2), 105-113.
- Erway L., Fraser A. S., and Hurley L. S. (1971) Prevention of Congenital Otolith Defect in Pallid Mutant Mice by Manganese Supplementation. *Genetics* **67**(1), 97-108.
- Erway L. C., Purichia N. A., Netzler E. R., Damore M. A., Esses D., and Levine M. (1986) Genes, Manganese, and Zinc in Formation of Otoconia - Labeling, Recovery, and Maternal Effects. *Scanning Electron Microscopy* **1986**, 1681-1694.
- Freeman C. L., Harding J. H., and Duffy D. M. (2008) Simulations of calcite crystallization on self-assembled monolayers. *Langmuir* **24**(17), 9607-9615.
- Halden N. M., Mathers K., Babaluk J. A., and Mejia S. R. (2004) Cathodoluminescence microscopy: A useful tool for assessing incremental chemical variation in otoliths. *Environmental Biology of Fishes* **71**(1), 53-61.
- Hori R. and Iwasaki S. (1976) Manganese Content of Egg of *Oryzias-Latipes* and its Changes During Early Development. *Protoplasma* **87**(4), 403-407.
- Hughes I., Blasiole L., Huss D., Warchol M. E., Rath N. P., Hurle B., Ignatova E., Dickman J. D., Thalmann R., Levenson R., and Ornitz D. M. (2004) Otopetrin 1 is required for otolith formation in the zebrafish *Danio rerio*. *Developmental Biology* **276**(2), 391-402.
- Jolivet A., Bardeau J. F., Fablet R., Paulet Y. M., and de Pontual H. (2008) Understanding otolith biomineralization processes: new insights into microscale spatial distribution of organic and mineral fractions from Raman microspectrometry. *Analytical and Bioanalytical Chemistry* **392**(3), 551-560.
- Kalish J. M. (1990) Use of Otolith Microchemistry to Distinguish the Progeny of Sympatric Anadromous and Non-Anadromous Salmonids. *Fishery Bulletin* **88**(4), 657-666.
- Kalish J. M., Beamish R. J., Brothers E. B., Casselman J. M., Francis R., Mosegaard H., Panfili J., Prince E. D., Thresher R. E., Wilson C. A., and Wright P. J. (1995) Glossary for otolith studies. In *Recent*

Developments in Fish Otolith Research (ed. D. H. Secor, J. M. Dean, and S. E. Campana), pp. 723-729.

Kudo M., Kameda J., Saruwatari K., Ozaki N., Okano K., Nagasawa H., and Kogure T. (2010) Microtexture of larval shell of oyster, *Crassostrea nippona*: A FIB-TEM study. *Journal of Structural Biology* **169**(1), 1-5.

Landtwing M. R. and Pettke T. (2005) Relationships between SEM-cathodoluminescence response and trace-element composition of hydrothermal vein quartz. *American Mineralogist* **90**(1), 122-131.

Li Z., Gao Y. H., and Feng Q. L. (2009) Hierarchical structure of the otolith of adult wild carp. *Materials Science & Engineering C-Biomimetic and Supramolecular Systems* **29**(3), 919-924.

Limburg K. E., Elfman M., Kristiansson P., Malmkvist K., and Pallon J. (2003) New insights into fish ecology via nuclear microscopy of otoliths. In *Application of Accelerators in Research and Industry*, Vol. 680 (ed. J. L. Duggan and I. L. Morgan), pp. 339-342. Amer Inst Physics.

Limburg K. E., Huang R., and Bilderback D. H. (2007) Fish otolith trace element maps: new approaches with synchrotron microbeam x-ray fluorescence. *X-Ray Spectrometry* **36**(5), 336-342.

Lowenstam H. A. (1981) Minerals Formed by Organisms. *Science* **211**(4487), 1126-1131.

Melancon S., Fryer B. J., Gagnon J. E., and Ludsins S. A. (2008) Mineralogical approaches to the study of biomineralization in fish otoliths. *Mineralogical Magazine* **72**(2), 627-637.

Miller J. A. and Kent A. J. R. (2009) The determination of maternal run time in juvenile Chinook salmon (*Oncorhynchus tshawytscha*) based on Sr/Ca and Sr-87/Sr-86 within otolith cores. *Fisheries Research* **95**(2-3), 373-378.

Murayama E., Okuno A., Ohira T., Takagi Y., and Nagasawa H. (2000) Molecular cloning and expression of an otolith matrix protein cDNA from the rainbow trout, *Oncorhynchus mykiss*. *Comparative Biochemistry and Physiology B-Biochemistry & Molecular Biology* **126**(4), 511-520.

Murayama E., Takagi Y., and Nagasawa H. (2004) Immunohistochemical localization of two otolith matrix proteins in the otolith and inner ear of the rainbow trout, *Oncorhynchus mykiss*: comparative aspects

- between the adult inner ear and embryonic otocysts. *Histochemistry and Cell Biology* **121**(2), 155-166.
- Murayama E., Takagi Y., Ohira T., Davis J. G., Greene M. I., and Nagasawa H. (2002) Fish otolith contains a unique structural protein, otolin-1. *European Journal of Biochemistry* **269**(2), 688-696.
- Nalla R. K., Porter A. E., Daraio C., Minor A. M., Radmilovic V., Stach E. A., Tomsia A. P., and Ritchie R. O. (2005) Ultrastructural examination of dentin using focused ion-beam cross-sectioning and transmission electron microscopy. *Micron* **36**(7-8), 672-680.
- Neumann M. and Epple M. (2007) Monohydrocalcite and its relationship to hydrated amorphous calcium carbonate in biominerals. *European Journal of Inorganic Chemistry*(14), 1953-1957.
- Pouget E. M., Bomans P. H. H., Goos J., Frederik P. M., de With G., and Sommerdijk N. (2009) The Initial Stages of Template-Controlled CaCO₃ Formation Revealed by Cryo-TEM. *Science* **323**(5920), 1455-1458.
- Rosauer E. A. and Redmond J. R. (1985) Comparative Crystallography of Vertebrate Otoconia. *Journal of Laryngology and Otology* **99**(1), 21-28.
- Ruttenberg B. I., Hamilton S. L., Hickford M. J. H., Paradis G. L., Sheehy M. S., Standish J. D., Ben-Tzvi O., and Warner R. R. (2005) Elevated levels of trace elements in cores of otoliths and their potential for use as natural tags. *Marine Ecology-Progress Series* **297**, 273-281.
- Saunders M., Kong C., Shaw J. A., Macey D. J., and Clode P. L. (2009) Characterization of biominerals in the radula teeth of the chiton, *Acanthopleura hirtosa*. *Journal of Structural Biology* **167**(1), 55-61.
- Secor D. H., Rooker J. R., Zlokovitz E., and Z. Danowicz V. S. (2001) Identification of riverine, estuarine, and coastal contingents of Hudson River striped bass based upon otolith elemental fingerprints. *Marine Ecology-Progress Series* **211**, 245-253.
- Sokolowski B. H. A. (1986) Development of the Otolith in Embryonic Fishes with Special Reference to the Toadfish, *Opsanus-Tau*. *Scanning Electron Microscopy* **1986**, 1635-1648.
- Sollner C., Burghammer M., Busch-Nentwich E., Berger J., Schwarz H., Riekel C., and Nicolson T. (2003) Control of crystal size and lattice formation by starmaker in otolith biomineralization. *Science* **302**(5643), 282-286.

- Stokes D. J., Morrissey F., and Lich B. H. (2006) A new approach to studying biological and soft materials using focused ion beam scanning electron microscopy (FIB SEM). In *EMAG-NANO 2005: Imaging, Analysis and Fabrication on the Nanoscale*, Vol. 26 (ed. P. D. Brown, R. Baker, and B. Hamilton), pp. 50-53.
- Templeton A. and Knowles E. (2009) Microbial Transformations of Minerals and Metals: Recent Advances in Geomicrobiology Derived from Synchrotron-Based X-Ray Spectroscopy and X-Ray Microscopy. *Annual Review of Earth and Planetary Sciences* **37**, 367-391.
- Thresher R. E. (1999) Elemental composition of otoliths as a stock delineator in fishes. *Fisheries Research* **43**(1-3), 165-204.
- Volk E. C., Blakley A., Schroder S. L., and Kuehner S. M. (2000) Otolith chemistry reflects migratory characteristics of Pacific salmonids: Using otolith core chemistry to distinguish maternal associations with sea and freshwaters. *Fisheries Research* **46**(1-3), 251-266.
- Warner R. R., Swearer S. E., Caselle J. E., Sheehy M., and Paradis G. (2005) Natal trace-elemental signatures in the otoliths of an open-coast fish. *Limnology and Oceanography* **50**(5), 1529-1542.
- Wirth R. (2009) Focused Ion Beam (FIB) combined with SEM and TEM: Advanced analytical tools for studies of chemical composition, microstructure and crystal structure in geomaterials on a nanometer scale. *Chemical Geology* **261**(3-4), 217-229.
- Zhang Z. and Beamish R. J. (2000) Use of otolith microstructure to study life history of juvenile Chinook salmon in the Strait of Georgia in 1995 and 1996. *Fisheries Research* **46**(1-3), 239-250.
- Zhang Z. and Runham N. W. (1992) Initial Development of *Oreochromis-Niloticus* (Teleostei, Cichlidae) Otolith. *Journal of Zoology* **227**, 465-478.

CHAPTER 2

A nano-scale chemical and structural characterization of Chinook salmon (*Oncorhynchus tshawytscha*) otolith cores using a FIB and HRTEM*

.

* This chapter incorporates the outcome of a joint research undertaken in collaboration with Dr. Joel Gagnon, Dr. Todd Simpson, and Dr. Christopher Weisener.

2.1 INTRODUCTION

Otoliths are found in the inner ear organs of teleost (bony) fish and are used for hearing and balance (PARKER, 1903; POPPER et al., 2003). Otoliths are composed of predominantly (~ 97 to 99%) calcium carbonate in the aragonite polymorph (CaCO_3) with an organic matrix containing glycoproteins, proteoglycans and collagens (~ 2 to 10%) (BORELLI et al., 2003; CARLSTROM, 1963; DEGENS et al., 1969; FERMIN et al., 1998; MURAYAMA et al., 2000; PISAM et al., 2002; TADASHI, 1996). Daily growth rings are formed in otoliths via the precipitation and accretion of organic and inorganic components from the endolymph fluid. During this process, trace amounts of other elements (up to 1.0 %) may substitute for calcium in the matrix and are thought to reflect ambient water chemistry (CAMPANA, 1999). The trace element composition is regarded by many as an environmental tracer and is typically analyzed using laser ablation inductively coupled plasma mass spectrometry (LA-ICP-MS) (CAMPANA, 1999). This method requires minimal sample preparation beyond initial polishing and sectioning of the otolith to produce a cross section and sonication to remove debris. Many studies have used LA-ICP-MS to examine the concentrations and spatial distribution of trace elements among several fish species across habitats (CAMPANA, 1999; THRESHER, 1999).

While the post-hatch region of the otolith reflects ambient chemistry during post-hatch life, the core region of the otolith, which is formed during

embryonic development, represents natal site chemistry as well as maternal associations (KALISH et al., 1995; VOLK et al., 2000). Typically less than 20 μm in diameter, the otolith core contains one or several primordia, which are the initial sites of otolith nucleation (0.5 to 1 μm diameter) (KALISH et al., 1995; MELANCON et al., 2008). Evidence suggests that the core is structurally and compositionally different from the post-hatch otolith, containing a higher organic content, an amorphous structure and manganese (Mn) enrichment (BEIER and ANKEN, 2006; BROPHY et al., 2004; CARLSTROM, 1963; JOLIVET et al., 2008; LOWENSTAM, 1981; MELANCON et al., 2008; MURAYAMA et al., 2004; NEUMANN and EPPLE, 2007; POUGET et al., 2009; RUTTENBERG et al., 2005; SOKOLOWSKI, 1986; ZHANG and RUNHAM, 1992).

Despite the strides made by these studies in identifying the organic constituents and general chemistry of the otolith, questions remain about the nano-scale chemistry of the otolith. This information is desirable because it can reveal the requirements for early development in fish. While LA-ICP-MS can be used to differentiate between the core and the post-hatch otolith based on Mn-enrichment in the core, laser spot size is variable, down to about 6 μm . With the average primordia being ~ 1 to 0.5 μm in diameter, LA-ICP-MS cannot provide a nano-scale chemical characterization of the otolith core. A high-resolution (i.e., nanometer) method that prevents or limits alteration of the sample structure and chemistry is needed in order to obtain information regarding the structure and composition of otolith cores. In this study, we combine a number of micro- and nano-scale sampling, imaging,

and analytical methods to obtain structural and compositional information from the post-hatch and core region of juvenile Chinook salmon (*Oncorhynchus tshawytscha*) otoliths. This information can provide a more accurate assessment of core chemistry that can in turn be used to better understand the early life history and maternal associations of fish stocks. The methods used include transmitted light microscopy, scanning electron microscopy (SEM), focused ion beam (FIB) milling and sectioning, and high resolution transmission electron microscopy (HRTEM).

2.2 MATERIALS AND METHODS

One of the challenges in this study was to precisely correlate micro-scale (e.g., otolith sectioning) and nano-scale (e.g., core/primordia sectioning) characterization and analysis while maintaining the ability to quickly and accurately relocate the same, nano-scale feature (i.e., primordia) within an otolith. To achieve this, a procedure was developed where a number of analytical methods were employed to spatially reference, sample and characterize otolith cores. In, summary, the procedure that was developed involved:

1. Extraction and sectioning of the otoliths.
2. Application of reference markings on the surface of the sectioned otolith using the FIB.

3. Identification and preliminary characterization of core regions and primordia using micro-scale methods, such as SEM-energy dispersive X-ray spectroscopy (SEM-EDS) and SEM cathodoluminescence (SEM-CL).
4. Thin sectioning and chemical and structural characterization using nano-scale methods (e.g., FIB and HRTEM).

2.2-1 Extraction and sectioning of otoliths

Otoliths from Chinook salmon fry harvested from Lake Ontario, Ontario, Canada, were extracted according to the method described by Payan et al. (1997). After extraction, otoliths were rinsed with Milli-Q[®] ultrapure water and sonicated for approximately five minutes in a closed Petrie dish in Milli-Q[®] water. Otoliths were then rinsed three times with Milli-Q[®] water, mounted on a glass microscope slide and embedded in Crystal Bond 509[®], a thermoplastic polymer. Otoliths were then polished using Milli-Q[®] water and 30-, 12- and 9-micron silica lapping film successively until the core region appeared to be exposed upon examination under a Nikon[®] polarizing light microscope in transmitted light.

2.2-2 Application of reference marks

A similar methodology of orienting the otoliths, along with the fact that they were of similar size (and age) prior to polishing made the location of the general core region relatively predictable. Through comparison with

annotated light micrographs highlighting the core region of individual samples, reference markings (a numbered and lettered grid) was machined onto the surface of the otolith using a FIB of gallium (Ga) ions to provide coordinates for the relocation of individual primordia within the otolith cores between analytical methods. Figure 1 is a secondary electron SEM image of the otolith showing the FIB-milled grid on the surface for relocation of the core during later FIB thin-sectioning. Application of the reference marks and subsequent sectioning was conducted using the Zeiss™ 1540XB FIB/SEM at the Western Nanofabrication Facility at the University of Western Ontario, London, Ontario, Canada. After reference markings were milled, preliminary characterization of the core was conducted at the Great Lakes Institute for Environmental Research, University of Windsor, Windsor, Ontario, Canada.

2.2-3 SEM-CL and SEM-EDS analysis

An FEI™ Quanta™ 200F field emission gun (FEG) SEM, equipped with CL, was used to obtain images (Centaurus® scintillator backscattered detector, high vacuum, 300 to 650 nm spectral range) of polished otoliths. SEM-CL was used because it is a non-destructive imaging technique that possesses several advantages over traditional CL, such as simultaneous EDS analysis, which enables the detection of variations in the concentrations of minor elements (LANDTWING and PETTKE, 2005). Sample slides were carbon-coated prior to imaging and affixed to the stage using double-sided,

conductive carbon tape. After primordia were located using CL, samples were re-imaged in backscattered electron (BSE) mode under low vacuum (~80 Pa). Low vacuum was used in SEM-BSE mode to optimize sample imaging by avoiding the excessive charging inherent to high vacuum analysis. The electron beam current was maintained between 10 to 20 kV to avoid beam damage. Spot size was ~ 3 nm. To determine the spatial distribution of elements within the otolith, elemental maps were collected and analyzed using an EDAX Sapphire Si(Li) EDS detector and Genesis™ v5.21 software. SEM-EDS provided elemental maps that were used to confirm the presence of Mn peaks and provide preliminary microchemical data prior to FIB sectioning and HRTEM microchemical analysis. Core locations were referenced relative to the reference markings previously micro-machined using a FIB.

2.2-4 FIB/SEM analysis

A FIB of 30 keV Ga ions was used to cut an ~ 250 nm thick section from the otolith core. A pair of trenches 60 μm x 30 μm was FIB-milled on either side of a 5 μm wide strip containing the otolith core (Figure 2a). The course milling used a 10 nA beam of 30 keV energy gallium (Ga) ions focused to a beam diameter of ~ 500 nm. Prior to milling, a band of platinum (Pt) 2 μm thick was FIB-deposited over the region of interest to provide a smooth protective surface layer.

The exposed cross-section was polished on both sides using a 1 nA Ga beam (30 keV energy, 100 nm diameter) while simultaneously imaging by SEM-BSE under high vacuum. Polishing was terminated once the otolith core was exposed and visible in the SEM image. The exposed otolith cross-section was imaged using a 5 nA beam of 10 keV electrons in SEM-BSE and an elemental map of the region was then acquired by EDS. Extended exposure to the electron beam caused visible damage to the region around the otolith (Figure 3a). The damaged layer was subsequently removed as the thin section was FIB-polished to a reduced thickness of 2.5 μm .

The thin section was separated from the remainder of the otolith on one side and at the bottom leaving the 40 μm x 20 μm x 2.5 μm thick piece of material attached on one side (Figure 2b). The tungsten (W) tip of an End Effector™ mounted in the Ascend® Instruments Extreme Access™ lift-out manipulator was FIB-milled to produce a pair of tines spaced 2.5 μm apart. After the tines were wedged over the fixed end of the lamella, the final end was detached by FIB milling and the lamella was lifted clear of the trench.

Prior to final thinning, the lamella was welded to the tungsten tip with FIB-deposited Pt to increase the stability of the specimen. The End Effector™ was then folded over to form a 3 mm TEM grid. The sample was then mounted vertically in a small vice on the sample stage of the FIB/SEM. This approach provided precise and stable positioning of the lamella for final polishing. The thickness of the lamella was reduced to approximately 1 μm using a 200 pA Ga beam focused to approximately 50 nm diameter.

Progress was monitored by simultaneous SEM imaging. The sample was then rotated to view the second side by SEM during the final thinning. A 20 μm wide region of the lamella, centered on the otolith core, was thinned by FIB milling using a 30 keV energy, 200 pA beam. The thinning process was terminated when the section reached a thickness of 250 nm, although ideal TEM thin-section thickness for nanoscale characterization of chemistry and structure is between 100 and 150 nm. Curling and buckling of the sample, which was observed during the later portion of the thinning process, may have been due to the higher organic content and variable concentrations of mineral and organic components. A similar extent of buckling and curling was not observed in the thin section extracted from a post-hatch region, which was possibly due to the fact that organic content occurs in concentrations typically below 0.2 to 10 % outside the core (DEGENS et al., 1969).

Prior to sectioning, pockets with a porous or hollowed-out appearance were observed in the core region beneath a cluster of primordia (Figure 3b). It is possible that the porous texture observed may be the result of lost organic content incurred due to the length of the sample storage period (>6 months). The observation of this texture solely in the core region after an extended period of storage may be due to the loss of organic content that may have been present at one time in the otolith core, as organic content degrades over time when not properly preserved (i.e. frozen or chemically preserved; preservation through freezing or other means were not used for these samples). No studies, to our knowledge, have been conducted on the

degradation of organic material in the otolith relative to storage time, so it is difficult to tell what potential impact the storage time had on the organic content in the sample. Curling and buckling of the thin section during late-stage FIB thinning may have occurred due to the presence of this porous region within the core.

2.2-5 HRTEM analysis

The FIB-milled sections were later retrieved and analyzed using an FEI™ Titan™ 80-300 Cubed HRTEM at McMaster University, Hamilton, Ontario, Canada. Bright field (BF) images and high angle annular dark field (HAADF) scanning TEM (STEM) images were collected at 300 kV. In addition, EDS spectra were collected in STEM mode with a probe size of 0.5 nm or less.

2.3 RESULTS

2.3-1 Identification and preliminary micro-scale chemical characterization of core region using SEM-CL and SEM-EDS

Growth structures (e.g., diurnal rings and primordia) were not observed using SEM-BSE across the exposed sample surface (Figure 4a, background). SEM-CL imaging, however, revealed concentric, daily growth increments surrounding several luminescent primordia, each of which was observed to be less than 5 μm in diameter (Figure 4b). The luminosity of the diurnal

decreased with distance from the core region. EDS line scans across the core region confirmed the presence of an Mn peak (Figure 4a), corresponding with the location of primordium P1 identified using SEM-CL (Figure 4b).

The visible appearance of growth structures using SEM-CL (that could not be observed using SEM-BSE) is likely due to the difference in the limits of detection between the two methods. CL is sensitive to trace elements, often in the parts per billion range (ppb), while SEM-BSE is not ideal for imaging organics because the elements that compose the majority of the sample (C,O) are of low atomic mass and do not produce as much backscatter as metals or samples with greater concentrations of heavy elements.

The Mn peak observed via SEM-EDS at primordia P1 (Figure 4a, foreground) is consistent with earlier research, which suggests that the luminescence observed in otoliths is related to an increased Mn concentration (HALDEN et al., 2004). While luminescence was observed in primordia P1 through P3 using SEM-CL, SEM-EDS line scans conducted through primordia P2 and P3 did not yield detectable Mn as observed with P1, which may be due to insufficient polishing resulting in the core not being exposed at the sample surface. This highlights a significant challenge encountered during otolith core/primordia analysis, as manual polishing is a very inefficient method for revealing the otolith core. Due to the manner in which the otolith grows (i.e., it accretes around the central core, which houses the primordia), it can appear as though the core is well-exposed when, in reality, it may still be covered by several 10s of microns of post-hatch otolith. In addition, it only

takes a few passes of manual polishing to remove the area of interest because the individual primordia are so small. Therefore, the success of SEM-CL imaging of primordia is highly dependent upon sample preparation. For example, Figure 5 shows luminescence of the otolith core from another polished otolith sample. Despite the luminescence observed in the core in Figure 5, SEM-EDS did not detect a Mn peak in the core.

Despite the challenges in initial sample preparation, SEM-CL was applied successfully in this study to identify growth textures in otoliths. Methods of exposing the otolith core more precisely are required for imaging.

2.3-2 Thin sectioning and preliminary micro-scale chemical characterization of core region using FIB/SEM

A thin section of 250 nm thickness is shown prior to extraction from the surrounding otolith in Figure 2a. The exposed surface of the thin section adjacent to the excavated trench was imaged *in situ* prior to extraction (Figure 2b) using SEM-BSE. SEM-BSE images (Figure 6a) show that the core region contains a number of primordia that are arranged in a cluster formation and are chemically heterogeneous. The core boundary and primordia appear brighter (Figure 6a), possibly due to higher concentrations of heavier elements (such as Mn) producing more backscattered electrons compared to the adjacent core regions; however this variation could be affected by

structural differences as well. EDS maps collected using a FIB/SEM showed that the concentrations of C and O were positively correlated in the exposed sample surface, however, a weak, negative correlation was observed between the concentrations of C and O relative to Ca at the core boundary (Figure 6b). Mn occurred in higher concentrations in the primordia relative to the surrounding otolith core region (Figure 6b).

There was some concern about the ability of a FIB to section heterogeneous specimens, such as otoliths, which consist of mixtures of relatively hard (e.g., mineral) and soft (e.g., protein) materials. For example, Stokes et al. (2006) observed some alteration at the interface between mineralized and biological materials after using a FIB in sample preparation. Although the majority of the otolith outside of the core contains relatively low concentrations (~ 0.2 to 10 %) of organic material, the core has been characterized as having a greater concentration of organic compounds (DEGENS et al., 1969; JOLIVET et al., 2008). FIB-related alteration at the core-otolith or core-primordia interface after sectioning was not observed, however, some damage to the sample surface was observed after SEM-EDS mapping (Figure 3a). This damaged material was removed by polishing with the FIB after SEM-EDS mapping to expose fresh, unaltered material for subsequent characterization.

2.3-3 Nano-scale characterization of otolith chemistry and structure using HRTEM

Two prepared thin sections were imaged and analyzed using HRTEM. The first thin section was created from the post-hatch otolith region and was ~ 200 nm thick. HAADF images of this thin section revealed rounded, lighter-coloured “nodules” less than 1 µm in diameter that can be assumed to have a greater concentration of heavy elements than the lighter adjacent areas (Figure 7a). EDS spectra were collected in STEM mode from the centre and edge of a nodule as well as from the surrounding adjacent region (Figure 7b).

EDS spectral analysis on the central region of the nodule showed silicon (Si) content was 5.67 times greater by weight (2.38 weight percent, spectrum 5) compared with the darker, adjacent region (0.42 weight percent, spectrum 7) (Table 1). Atomic and weight percent values for all elements within the detection range at each spectral analysis location can be found in Table 1. The function of Si in otoliths and many other biominerals is not well understood, although in diatoms and sponges it is a major structural component and it plays a vital role in the formation of connective tissue in the bones and cartilage of mammals and birds (CARLISLE, 1988; PERRY, 2003).

D-spacings calculated from HRTEM images showed that the first thin section (milled from the post-hatch region) was composed of CaCO₃ in the aragonite polymorph. Measured d-spacing values were consistent at several locations, suggesting little structural and compositional variation throughout

the thin section. D-spacing values and fast Fourier transform (FFT) images for this thin section are included in Table 2 and Figure 8, respectively.

The second thin section was milled to include the core region of the otolith. TEM bright field (BF) images confirmed that this thin section contained several primordia (Figure 9a). High resolution images were collected from the regions indicated in Figure 9a. Figure 9b shows an interface between a primordium and the surrounding core region. While d-spacings could be calculated from a few regions of this thin-section where a crystalline structure was observed in the HRTEM images (and subsequently interpreted to be a relatively close match with aragonite, see Table 3), several regions were amorphous and d-spacings could not be calculated. Other regions where FFT was attempted (site 5-1 in Figure 9a) did not yield d-spacings consistent with any CaCO_3 polymorph (Table 3 and Figure 10). The more amorphous structure observed in the interface region and region 5-1, along with the darker appearance, suggests that both regions possess a composition more enriched in heavy elements compared with the region in 5-2. While darker contrast in TEM-BF can be suggestive of a physically thicker region, the close proximity of sites 5-1 and 5-2 ($< 25 \text{ nm}$) make variations in thickness an unlikely cause for the observed contrast (Figure 9b).

Our findings corroborate numerous prior studies that have suggested that the otolith core has a more amorphous structure than the post-hatch otolith, possibly due to the increased presence of amorphous CaCO_3 , or ACC (FREEMAN et al., 2008; LOWENSTAM, 1981; NEUMANN and EPPLE, 2007;

POUGET et al., 2009; SOKOLOWSKI, 1986). Thin sections in this study were milled from fry-aged (< 6 months old) otoliths. Juvenile otoliths are thought to retain a greater portion of ACC in the core than adult otoliths; therefore, variation of the degree of crystallinity in the otolith with age would likely be observed (SOKOLOWSKI, 1986). The amorphous regions observed in bright field TEM images (Figure 8) could also be reflective of increased organic content in the core from the presence of proteins necessary for the initiation and facilitation of mineralization in the otolith (BELCHER et al., 1996; KANG et al., 2008; SOLLNER et al., 2003).

EDS spectra were also collected on a single primordium to reveal the distribution of major element constituents (C, O, Ca) along with Mn. EDS results showed less C, Ca and O in the primordium relative to the adjacent core region (Figure 11). Mn, however, appears to be the most concentrated in the centre of the primordium and to a lesser degree in the surrounding interface between the primordium and core areas (Figure 11). EDS spectra collected from these regions, denoted in Figure 11, suggest the formation of several chemical gradients. In region 2, located in the central primordium, 3.3% Mn by weight is observed, while no Mn was detected in regions 5, 8 and 9, which are located outside the primordium. Additionally, regions 6 and 7, analyzed within the interface region between the primordium and the otolith core, had an average of 0.67% Mn by weight. A summary of the weight and atomic percent values for all elements are shown in Table 4.

2.4 DISCUSSION

These findings agree with those of previous otolith microchemistry studies, which detected Mn peaks within the centre of otolith cores of various species (BROPHY et al., 2004; MELANCON et al., 2008; RUTTENBERG et al., 2005). This study, however, further constrains the localization of Mn on the nano-scale by identifying Mn peak concentrations first to be concentrated within primordia, via SEM-EDS, then to the core-primordia interface and central primordia region via STEM. Due to thickness of the sample it was not possible to acquire the highest resolution TEM images possible, which would provide greater nano-scale insight into the localization of Mn within the otolith primordia. In addition, it is also unclear the effects that storage time may have had on the organic content and localization of Mn within the otolith. Future studies should attempt to obtain thinner sections, approximately 100 to 150 nm thick, in order to obtain more nano-scale chemical data. A positive correlation between increased concentrations of Mn in the embryo and healthy development and growth processes has been observed in several species (ERWAY et al., 1971; ERWAY et al., 1986; HORI and IWASAKI, 1976). Studies of Mn deficiencies in mice, rats, guinea pigs, and chicks showed deficiency led to several severe otoconial defects, such as a reduction in size, or absence altogether (ERWAY et al., 1971; ERWAY et al., 1986). It is possible, based on evidence from this study, that the presence of Mn is vital for early development of otoliths in teleosts as well. These findings are consistent with

previous findings that indicate the preferential incorporation of Mn into the pre-hatch otolith is primarily facilitated by the mother or due to early developmental requirements (maternal associations), rather than as a result of environmental influences (MELANCON et al., 2008). These data suggest that the otolith core and primordia are not chemically, structurally, or mechanistically uniform. Reconstructions of life history and natal habitats of fish using otolith chemistry must be conducted with knowledge of the incongruencies between the pre- and post-hatch otolith, and the preferential incorporation of Mn during early development in the otolith. A FIB, in conjunction with high-resolution methods such as HRTEM, or perhaps synchrotron, provides a bridge to the nanoscale, allowing researchers to delve into the chemistry of embryonic development.

2.5 LITERATURE CITED

- Beier M. and Anken R. (2006) On the role of carbonic anhydrase in the early phase of fish otolith mineralization. In *Space Life Sciences*, Vol. 38 (ed. L. L. Bruce and C. Dournon), pp. 1119-1122.
- Belcher A. M., Wu X. H., Christensen R. J., Hansma P. K., Stucky G. D., and Morse D. E. (1996) Control of crystal phase switching and orientation by soluble mollusc-shell proteins. *Nature* **381**(6577), 56-58.
- Borelli G., Mayer-Gostan N., Merle P. L., De Pontual H., Boeuf G., Allemand D., and Payan P. (2003) Composition of biomineral organic matrices with special emphasis on turbot (*Psetta maxima*) otolith and endolymph. *Calcified Tissue International* **72**(6), 717-725.
- Brophy D., Jeffries T. E., and Danilowicz B. S. (2004) Elevated manganese concentrations at the cores of clupeid otoliths: possible environmental, physiological, or structural origins. *Marine Biology* **144**(4), 779-786.
- Campana S. E. (1999) Chemistry and composition of fish otoliths: pathways, mechanisms and applications. *Marine Ecology-Progress Series* **188**, 263-297.
- Carlisle E. M. (1988) Silicon as a Trace Nutrient. *Science of the Total Environment* **73**(1-2), 95-106.
- Carlstrom D. (1963) A Crystallographic Study of Vertebrate Otoliths. *Biological Bulletin* **125**(3), 441-463.
- Degens E. T., Deuser W. G., and Haedrich R. L. (1969) Molecular Structure and Composition of Fish Otoliths. *Marine Biology* **2**(2), 105-113.
- Erway L., Fraser A. S., and Hurley L. S. (1971) Prevention of Congenital Otolith Defect in Pallid Mutant Mice by Manganese Supplementation. *Genetics* **67**(1), 97-108.
- Erway L. C., Purichia N. A., Netzler E. R., Damore M. A., Esses D., and Levine M. (1986) Genes, Manganese, and Zinc in Formation of Otoconia - Labeling, Recovery, and Maternal Effects. *Scanning Electron Microscopy* **1986**, 1681-1694.
- Fermin C. D., Lychakov D., Campos A., Hara H., Sondag E., Jones T., Jones S., Taylor M., Meza-Ruiz G., and Martin D. S. (1998) Otoconia biogenesis, phylogeny, composition and functional attributes. *Histology and Histopathology* **13**(4), 1103-1154.

- Freeman C. L., Harding J. H., and Duffy D. M. (2008) Simulations of calcite crystallization on self-assembled monolayers. *Langmuir* **24**(17), 9607-9615.
- Halden N. M., Mathers K., Babaluk J. A., and Mejia S. R. (2004) Cathodoluminescence microscopy: A useful tool for assessing incremental chemical variation in otoliths. *Environmental Biology of Fishes* **71**(1), 53-61.
- Hori R. and Iwasaki S. (1976) Manganese Content of Egg of *Oryzias-Latipes* and Its Changes During Early Development. *Protoplasma* **87**(4), 403-407.
- Jolivet A., Bardeau J. F., Fablet R., Paulet Y. M., and de Pontual H. (2008) Understanding otolith biomineralization processes: new insights into microscale spatial distribution of organic and mineral fractions from Raman microspectrometry. *Analytical and Bioanalytical Chemistry* **392**(3), 551-560.
- Kalish J. M., Beamish R. J., Brothers E. B., Casselman J. M., Francis R., Mosegaard H., Panfili J., Prince E. D., Thresher R. E., Wilson C. A., and Wright P. J. (1995) Glossary for otolith studies. In *Recent Developments in Fish Otolith Research* (ed. D. H. Secor, J. M. Dean, and S. E. Campana), pp. 723-729.
- Kang Y. J., Stevenson A. K., Yau P. M., and Kollmar R. (2008) Sparc Protein Is Required for Normal Growth of Zebrafish Otoliths. *Jaro-Journal of the Association for Research in Otolaryngology* **9**(4), 436-451.
- Landtwing M. R. and Pettke T. (2005) Relationships between SEM-cathodoluminescence response and trace-element composition of hydrothermal vein quartz. *American Mineralogist* **90**(1), 122-131.
- Lowenstam H. A. (1981) Minerals Formed by Organisms. *Science* **211**(4487), 1126-1131.
- Melancon S., Fryer B. J., Gagnon J. E., and Ludsins S. A. (2008) Mineralogical approaches to the study of biomineralization in fish otoliths. *Mineralogical Magazine* **72**(2), 627-637.
- Murayama E., Okuno A., Ohira T., Takagi Y., and Nagasawa H. (2000) Molecular cloning and expression of an otolith matrix protein cDNA from the rainbow trout, *Oncorhynchus mykiss*. *Comparative Biochemistry and Physiology B-Biochemistry & Molecular Biology* **126**(4), 511-520.

- Murayama E., Takagi Y., and Nagasawa H. (2004) Immunohistochemical localization of two otolith matrix proteins in the otolith and inner ear of the rainbow trout, *Oncorhynchus mykiss*: comparative aspects between the adult inner ear and embryonic otocysts. *Histochemistry and Cell Biology* **121**(2), 155-166.
- Neumann M. and Epple M. (2007) Monohydrocalcite and its relationship to hydrated amorphous calcium carbonate in biominerals. *European Journal of Inorganic Chemistry*(14), 1953-1957.
- Parker G. H. (1903) The Sense of Hearing in Fishes. *The American Naturalist* **37**(435), 185-204.
- Payan P., Kossmann H., Watrin A., Mayer-Gostan N., and Boeuf G. (1997) Ionic composition of endolymph in teleosts: origin and importance of endolymph alkalinity. *J Exp Biol* **200**(13), 1905-1912.
- Perry C. C. (2003) Silicification: The processes by which organisms capture and mineralize silica. In *Biomineralization*, Vol. 54 (ed. P. M. Dove, J. J. DeYoreo, and S. Weiner), pp. 291-327.
- Pisam M., Jammet C., and Laurent D. (2002) First steps of otolith formation of the zebrafish: role of glycogen? *Cell and Tissue Research* **310**(2), 163-168.
- Popper A. N., Fewtrell J., Smith M. E., and McCauley R. D. (2003) Anthropogenic sound: Effects on the behavior and physiology of fishes. *Marine Technology Society Journal* **37**(4), 35-40.
- Pouget E. M., Bomans P. H. H., Goos J., Frederik P. M., de With G., and Sommerdijk N. (2009) The Initial Stages of Template-Controlled CaCO₃ Formation Revealed by Cryo-TEM. *Science* **323**(5920), 1455-1458.
- Ruttenberg B. I., Hamilton S. L., Hickford M. J. H., Paradis G. L., Sheehy M. S., Standish-J. D., Ben-Tzvi O., and Warner R. R. (2005) Elevated levels of trace elements in cores of otoliths and their potential for use as natural tags. *Marine Ecology-Progress Series* **297**, 273-281.
- Sokolowski B. H. A. (1986) Development of the Otolith in Embryonic Fishes with Special Reference to the Toadfish, *Opsanus-Tau*. *Scanning Electron Microscopy* **1986**, 1635-1648.
- Sollner C., Burghammer M., Busch-Nentwich E., Berger J., Schwarz H., Riekel C., and Nicolson T. (2003) Control of crystal size and lattice

formation by starmaker in otolith biomineralization. *Science* **302**(5643), 282-286.

Stokes D. J., Morrissey F., and Lich B. H. (2006) A new approach to studying biological and soft materials using focused ion beam scanning electron microscopy (FIB SEM). In *EMAG-NANO 2005: Imaging, Analysis and Fabrication on the Nanoscale*, Vol. 26 (ed. P. D. Brown, R. Baker, and B. Hamilton), pp. 50-53.

Tadashi S., Mugiya Y. (1996) Biochemical properties of water-soluble otolith proteins and the immunobiochemical detection of the proteins in serum and various tissues in the tilapia *Oreochromis niloticus*. *Fisheries Science* **62**, 970-976.

Thresher R. E. (1999) Elemental composition of otoliths as a stock delineator in fishes. *Fisheries Research* **43**(1-3), 165-204.

Volk E. C., Blakley A., Schroder S. L., and Kuehner S. M. (2000) Otolith chemistry reflects migratory characteristics of Pacific salmonids: Using otolith core chemistry to distinguish maternal associations with sea and freshwaters. *Fisheries Research* **46**(1-3), 251-266.

Zhang Z. and Runham N. W. (1992) Initial Development of *Oreochromis-Niloticus* (Teleostei, Cichlidae) Otolith. *Journal of Zoology* **227**, 465-478.

CHAPTER 3

Summary, suggestions for future work and conclusions

3.1 SUMMARY

This study employed a number of micro- and nano-scale techniques to develop a methodology for the preparation of otolith thin sections using a FIB and subsequent characterization using HTEM. Otoliths were first polished and a numbered grid was FIB-milled onto the sample surface to assist with re-locating regions of interest (i.e. core, or individual primordia). SEM-CL and SEM-EDS were then used to image the otolith and identify the core based on the luminescence of Mn.

The otolith core was then relocated using the previously FIB-milled grid under SEM-BSE and a thin section of ~ 250 nm was FIB-milled and included the otolith core region. An additional thin section (~ 200 nm thick) was milled from a region of the post-hatch otolith. D-spacings collected using FFT of HTEM images revealed that the thin-section from the post-hatch otolith was composed of aragonite while the inability to collect many d-spacings from the core suggested a more amorphous structure, perhaps due to presence of ACC or more protein.

EDS conducted on the post-hatch otolith section showed Si-enriched nodules were present (5.67 times more Si by weight in nodules compared to adjacent area). In the core thin section, EDS showed less C, Ca and O in the primordia relative to the remainder of the core. Increased concentrations of Mn were constrained through SEM and HTEM to the centre of the primordia and at the core-primordia interface (3.3% and 0.67% by weight, respectively).

3.2 SUGGESTIONS FOR FUTURE WORK

Future work should focus on increasing the number of thin sections in order to definitively constrain the microchemistry of the post-hatch otolith and the core. In light of the difficulties faced in this study related to sample fragility, future studies should also examine the potential effects of storage time on structure and organic content in otoliths as samples used in this study had a relatively long period of storage (> 6 months). Frozen samples, or those with a shorter storage period, could retain more organic content, allowing them to be more stable during thinning of the section, although this assertion is speculative. Thinner sections (100 to 150 nm), used in conjunction with HTEM or synchrotron, could provide more high-resolution images than we were able to obtain in this study. Future work could also produce thin-sections from the otoliths of other teleost species, in particular, those with a single primordium. These studies could examine any differences in the structure or chemistry across life stages due to storage and allow for comparison with species that have multiple primordia.

Other suggestions for future work relate to the preparatory steps necessary for the exposure of the core prior to sectioning. While our use of SEM-CL builds on the work of others who have used this technique to identify growth textures in otoliths (BEAREZ, 2005; HALDEN, 2004), exposure of the otolith core continues to be a challenge and more accurate methods of

polishing otoliths are desirable. The use of a FIB for this type of polishing has yet to be evaluated. Future studies could examine the feasibility of FIB polishing as a method for exposing the core and/or other features of the otolith.

3.3 CONCLUSIONS

The goals of this study were to 1) examine the possibility of using a FIB in conjunction with SEM to create thin-sections from the otolith and if successful, 2) to conduct a nano-scale characterization of chemistry and structure of the post-hatch otolith and the otolith core. As discussed in Chapter two, we found that the use of a FIB and SEM proved to be an effective method for the production of thin sections from the otolith. This study also successfully conducted EDS and collected d-spacings from both thin sections to characterize the chemistry and structure of the two samples.

The implications of the use of a FIB/SEM set-up in the field of otolith research can be surmised based on its now widespread use among other biominerals (KUDO et al., 2010; MACLEAN et al., 2008; NALLA et al., 2005; SAUNDERS et al., 2009). The use of a FIB allows researchers the ability to create a sample that can be used in conjunction with high resolution microscopy in the investigation of the complex organic-inorganic matrices associated with biominerals. The relative ease with which thin-sections can be created from otoliths using a FIB should also be emphasized when citing

its widespread usage. While samples in this study were polished and sectioned beforehand, it is not a necessary step, *per se*. It would only be when the aim is to create a thin-section from a particular feature of the otolith (e.g., a certain region of growth, or from the core), that more complex sample preparation is required prior to FIB sectioning (e.g., polishing, SEM-CL identification of the core).

Despite some limitations encountered during the project, data obtained from the use of this methodology reveals new information about otolith chemistry and structure on the nano-scale. The identification of Si-enriched nodules in the post-hatch otolith, and Mn localizations in specific regions of the core, suggests that there are nano-scale localizations of elements in otoliths. The mechanism by which certain elements might be enriched in particular regions of the otolith is not understood, but these data provide more evidence that some aspects of the incorporation of elements in the otolith is not a simple process. The occurrence of these locally-enriched areas is likely not reflective of the ambient environment, but rather, linked to some role in mineralization or development.

In particular, the finding that Mn is actually localized specifically in the central and primordia-core interface regions, provides further evidence for the importance of Mn in the early formation of otoliths. Other studies have already found that without sufficient Mn, otoconia in other species are malformed or absent altogether (ERWAY et al., 1971; ERWAY et al., 1986). Since previous studies have provided evidence that Mn-enrichment is from

maternal/early development processes (MELANCON et al., 2008), rather than from environmental enrichment, it raises the question that if Mn were found to be deficient in the maternal contribution (yolk sac), would otoliths form properly? Based on the findings of this study, which constrain Mn enrichment particularly to the center of the primordia, it seems a realistic assumption that Mn is required for the proper development of otoliths and the subsequent survival of the individual.

3.4 LITERATURE CITED

- Bearez P., Carlier G., Lorand J. P., and Parodi G. C. (2005) Destructive and non-destructive microanalysis of biocarbonates applied to anomalous otoliths of archaeological and modern *sciaenids* (Teleostei) from Peru and Chile. *Comptes Rendus Biologies* **328**(3), 243-252.
- Erway L., Fraser A. S., and Hurley L. S. (1971) Prevention of Congenital Otolith Defect in Pallid Mutant Mice by Manganese Supplementation. *Genetics* **67**(1), 97-108.
- Erway L. C., Purichia N. A., Netzler E. R., Damore M. A., Esses D., and Levine M. (1986) Genes, Manganese, and Zinc in Formation of Otoconia - Labeling, Recovery, and Maternal Effects. *Scanning Electron Microscopy* **1986**, 1681-1694.
- Halden N. M., Mathers K., Babaluk J. A., and Mejia S. R. (2004) Cathodoluminescence microscopy: A useful tool for assessing incremental chemical variation in otoliths. *Environmental Biology of Fishes* **71**(1), 53-61.
- Kudo M., Kameda J., Saruwatari K., Ozaki N., Okano K., Nagasawa H., and Kogure T. (2010) Microtexture of larval shell of oyster, *Crassostrea nippona*: A FIB-TEM study. *Journal of Structural Biology* **169**(1), 1-5.
- Macleane L. C. W., Tyliszczak T., Gilbert P., Zhou D., Pray T. J., Onstott T. C., and Southam G. (2008) A high-resolution chemical and structural study of framboidal pyrite formed within a low-temperature bacterial biofilm. *Geobiology* **6**(5), 471-480.
- Melancon S., Fryer B. J., Gagnon J. E., and Ludsing S. A. (2008) Mineralogical approaches to the study of biomineralization in fish otoliths. *Mineralogical Magazine* **72**(2), 627-637.
- Nalla R. K., Porter A. E., Daraio C., Minor A. M., Radmilovic V., Stach E. A., Tomsia A. P., and Ritchie R. O. (2005) Ultrastructural examination of dentin using focused ion-beam cross-sectioning and transmission electron microscopy. *Micron* **36**(7-8), 672-680.
- Saunders M., Kong C., Shaw J. A., Macey D. J., and Clode P. L. (2009) Characterization of biominerals in the radula teeth of the chiton, *Acanthopleura hirtosa*. *Journal of Structural Biology* **167**(1), 55-61.

Table 1.

EDS spectra collected via HRTEM from otolith nodules, outside otolith core.
Table A includes elements analyzed in atomic %; Table B includes elements analyzed in weight %.

A)

All elements analyzed (Normalized)

Spectrum	In stats.	C	O	Mg	Si	P	Ca	Mn
Spectrum 1	No	23.21	53.07	0.00	0.45	0.03	23.35	0.00
Spectrum 2	No	21.00	46.97	0.00	1.13	0.04	31.17	0.00
Spectrum 3	No	23.51	53.18	0.00	0.53	0.02	22.89	0.00
Sum	No	33.31	46.17	0.00	0.61	0.03	19.98	0.00
Spectrum								
Spectrum 5	Yes	37.35	43.05	0.00	1.61	0.36	18.00	0.00
Spectrum 6	Yes	37.09	43.52	0.00	0.61	1.01	18.85	0.00
Spectrum 7	Yes	38.42	42.88	0.00	0.28	0.70	17.59	0.00
Mean		37.62	43.15	0.00	0.84	0.69	18.14	0.00
Std. deviation		0.70	0.33	0.00	0.69	0.33	0.64	0.00
Max.		38.42	43.52	0.00	1.61	1.01	18.85	0.00
Min.		37.09	42.88	0.00	0.28	0.36	17.59	0.00

All results in atomic%

B)

All elements analyzed (Normalized)

Spectrum	In stats.	C	O	Mg	Si	P	Ca	Mn	Total
Spectrum 1	Yes	13.44	40.92	0.00	0.61	0.05	45.10	0.00	100.00
Spectrum 2	Yes	11.07	32.99	0.00	1.40	0.05	54.84	0.00	100.00
Spectrum 3	Yes	13.69	41.24	0.00	0.73	0.03	44.46	0.00	100.00
Sum	Yes	20.46	37.78	0.00	0.87	0.05	40.96	0.00	100.00
Spectrum									
Spectrum 5	Yes	23.54	36.15	0.00	2.38	0.58	37.86	0.00	100.00
Spectrum 6	Yes	23.30	36.42	0.00	0.90	1.63	39.50	0.00	100.00
Spectrum 7	Yes	24.47	36.38	0.00	0.42	1.15	37.38	0.00	100.00
Mean		18.57	37.41	0.00	1.04	0.51	42.87	0.00	100.00
Std. deviation		5.66	2.90	0.00	0.66	0.65	6.07	0.00	
Max.		24.47	41.24	0.00	2.38	1.63	54.84	0.00	
Min.		11.07	32.99	0.00	0.42	0.03	37.38	0.00	

All results in weight%

Table 2.

D-spacing values calculated from HRTEM images on a thin section milled from outside the core region.

Sample Code	Image #	Live FFT location	$d_1(A)$	$d_1(A)$	$d_1(A)$	$d_1(A)$ peak matches	$d_1(A)$ peak matches	$d_1(A)$ peak matches
TEST	HR-1	1	2.77	2.35	2.17	012	112	122
TEST	HR-2	3	2.16	2.80	2.45	122	111	200
TEST	HR4	1	2.93	2.07	2.84	111	221	021
TEST	HR4	2	2.93	2.13	2.84	111	221	021
TEST	HR4	3	3.02	2.07	2.84	111	221	021
TEST	HR5	1	2.93	2.13	2.84	111	221	021
TEST	HR5	2	3.02	2.07	2.84	111	221	021
TEST	HR5	3	3.02	2.07	2.84	111	221	021

Table 3.

D-spacing values calculated from HRTEM images on a thin section milled from inside the core region.

Sample Code	Image #	Live FFT location	$d_1(A)$	$d_1(A)$	$d_1(A)$	$d_1(A)$ peak matches	$d_1(A)$ peak matches	$d_1(A)$ peak matches
S-1	HR-5	1	2.13	2.58	1.64	No close matches	No close matches	No close matches
S-1	HR-5	2	4.2	2.51	3.17	111	012	021
S-1	HR-6	1	2.13	2.58	2.61	221	200	012
S-1	HR-12	1	2.11	2.58	2.67	221	200	012

Table 4.

TEM-EDS spectra collected from multiple sites within the otolith primordia.
Table A includes elements analyzed in atomic %; Table B includes elements analyzed in weight %.

A)

All elements analyzed (Normalized)

Spectrum	In stats.	C	O	Mg	Si	P	Ca	Mn
Sum	Yes	23.53	47.97	0.29	0.27	0.16	27.57	0.20
Spectrum 2	Yes	24.32	48.17	0.13	0.20	0.65	25.24	1.29
Spectrum 3	Yes	18.40	51.61	0.45	0.57	0.37	28.34	0.26
Spectrum 4	Yes	23.37	48.44	0.51	0.59	0.22	26.39	0.47
Spectrum 5	Yes	24.72	47.91	0.00	0.17	0.00	27.56	0.00
Spectrum 6	Yes	22.27	46.86	0.45	0.52	0.37	29.34	0.18
Spectrum 7	Yes	27.20	41.32	0.55	0.38	0.41	29.77	0.36
Spectrum 8	Yes	20.62	48.26	0.10	0.00	0.30	30.90	0.04
Spectrum 9	Yes	27.54	47.31	0.09	0.74	0.00	24.76	0.00
Mean		23.55	47.54	0.26	0.36	0.23	27.76	0.30
Std. deviation		2.91	2.69	0.27	0.29	0.31	2.06	0.41
Max.		27.54	51.61	0.55	0.74	0.65	30.90	1.29
Min.		18.40	41.32	0.00	0.00	0.00	24.76	0.00

All results in atomic%

B)

All elements analyzed (Normalized)

Spectrum	In stats.	C	O	Mg	Si	P	Ca	Mn	Total
Sum	Yes	12.93	35.11	0.33	0.34	0.23	50.56	0.50	100.00
Spectrum 2	Yes	13.43	35.44	0.15	0.25	0.93	46.52	3.27	100.00
Spectrum 3	Yes	9.89	36.95	0.49	0.71	0.51	50.82	0.64	100.00
Spectrum 4	Yes	12.91	35.63	0.57	0.77	0.31	48.62	1.20	100.00
Spectrum 5	Yes	13.74	35.46	0.00	0.22	0.00	51.09	0.00	100.00
Spectrum 6	Yes	11.94	33.46	0.48	0.66	0.52	52.49	0.44	100.00
Spectrum 7	Yes	14.60	29.54	0.60	0.48	0.57	53.32	0.89	100.00
Spectrum 8	Yes	10.93	34.08	0.11	0.00	0.41	54.66	0.09	100.00
Spectrum 9	Yes	15.84	36.24	0.11	1.00	0.00	47.51	0.00	100.00
Mean		12.91	34.66	0.28	0.46	0.31	50.62	0.76	100.00
Std. deviation		1.81	2.18	0.30	0.38	0.45	2.69	1.04	
Max.		15.84	36.95	0.60	1.00	0.93	54.66	3.27	
Min.		9.89	29.54	0.00	0.00	0.00	46.52	0.00	

All results in weight%

Figure 1.

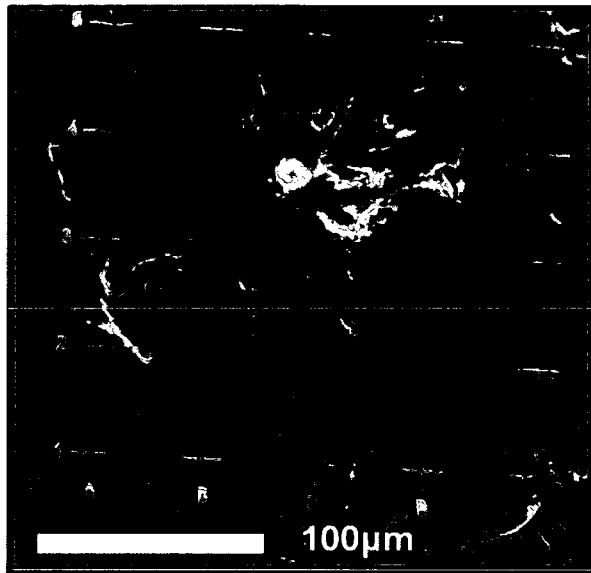


Figure 1: SEM-SE (secondary electron) image of sample surface with FIB-milled grid around the otolith core.

Figure 2.

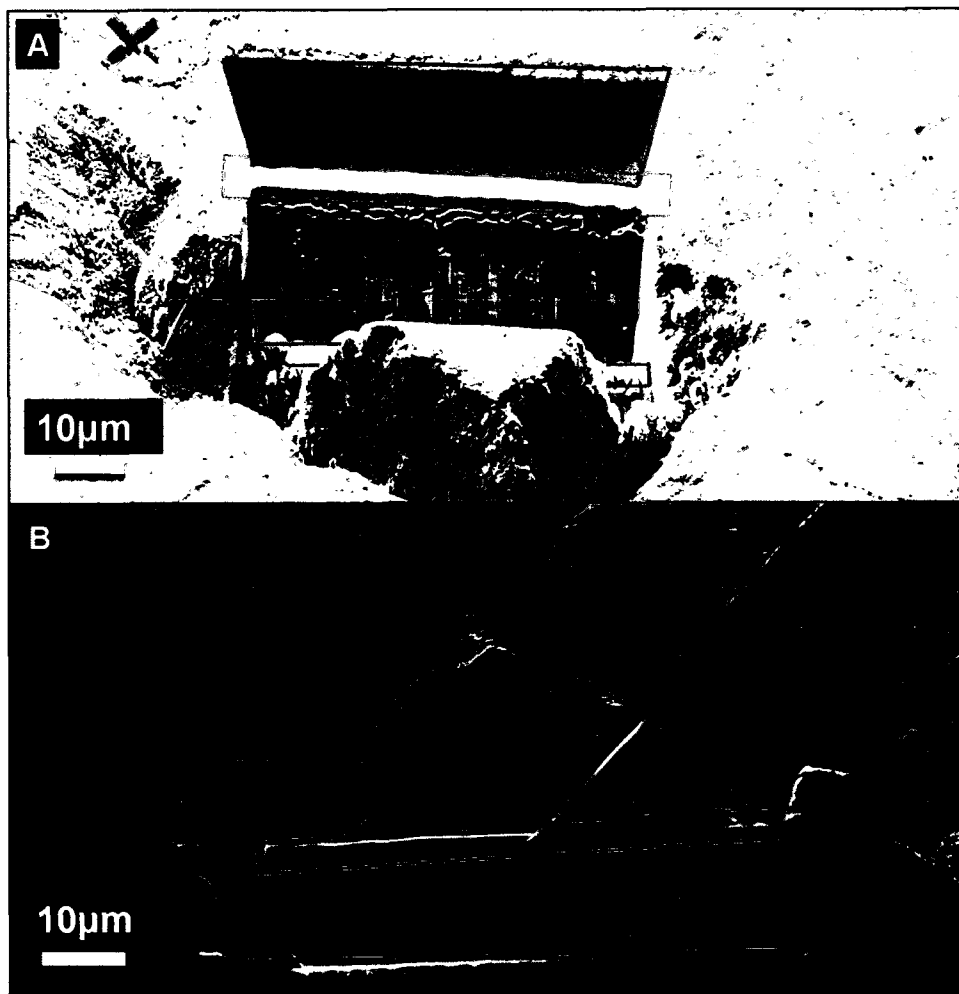


Figure 2: (A) SEM-SE image of two trenches (red) milled using a FIB on either side of the created thin section (top highlighted in purple) prior to lift-out. (B) Thin-section (highlighted in purple) lift-out using a pair of tines cut in the tip of a TEM grid-sized Mo foil. Edges of milled trenches denoted in red.

Figure 3.

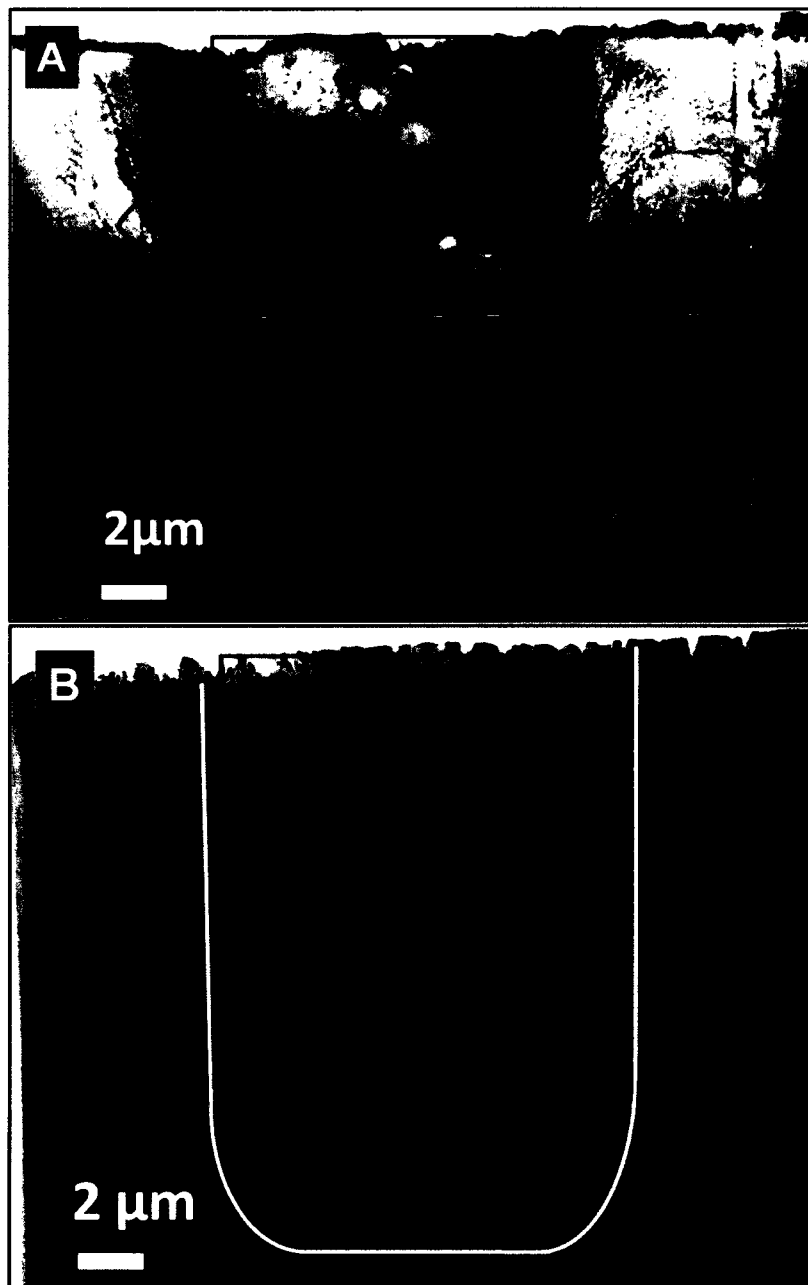


Figure 3: (A) SEM-BSE image of otolith core region after collection of SEM-EDS maps. Examples of beam damage can be observed in red bracketed regions. Primordia cluster is observed within purple boxed region. (B) SEM BSE image of core region prior to SEM-EDS mapping. The “porous” region in the green box observed just below the cluster of primordia (purple boxed regions, denoted by “P”) is possibly due to a loss of organic content during storage. The core boundary is denoted by the white line.

Figure 4.

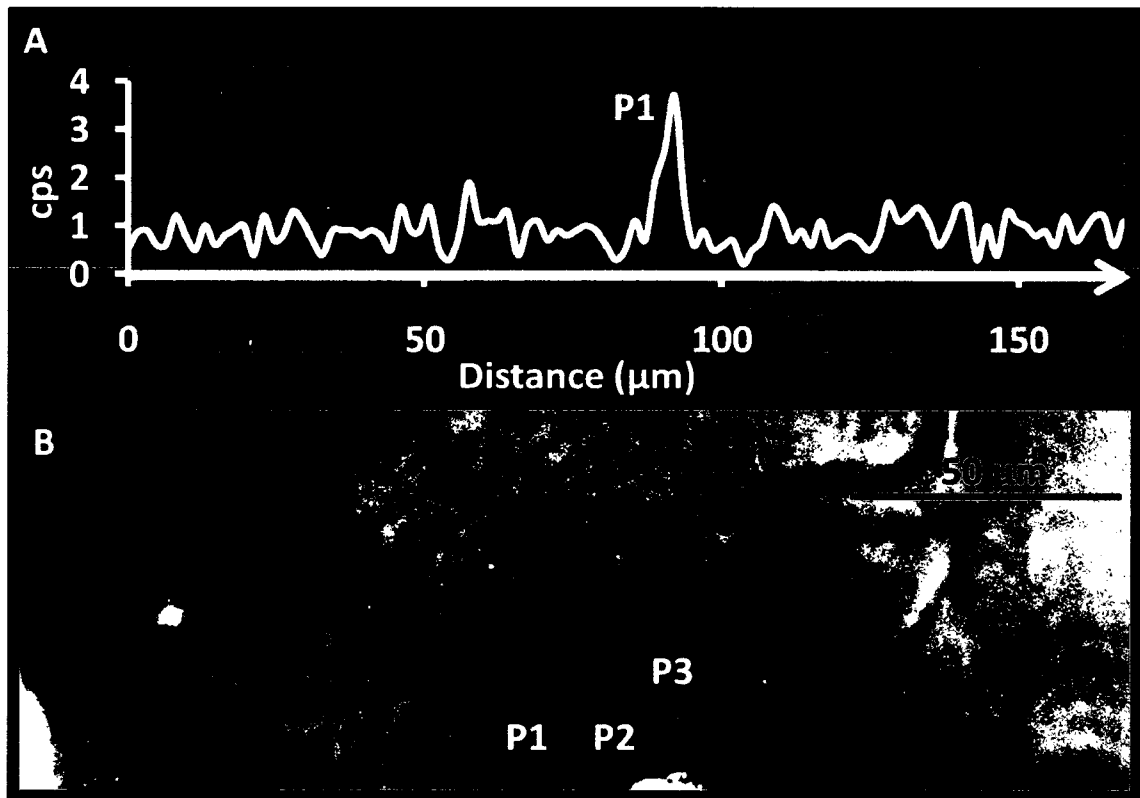


Figure 4: (A) (Background) SEM-BSE image of sample surface; (Foreground) The distribution of manganese (cps) across SEM-EDS line scan region (data taken along white arrow) where 'P1' denotes Mn peak associated with primordia location P1 in (B). (B) SEM-CL image of region shown in Figure 4A. Daily increments are visible occurring in concentric bands surrounding a central core region housing three luminescent primordia (P1-3).

Figure 5.

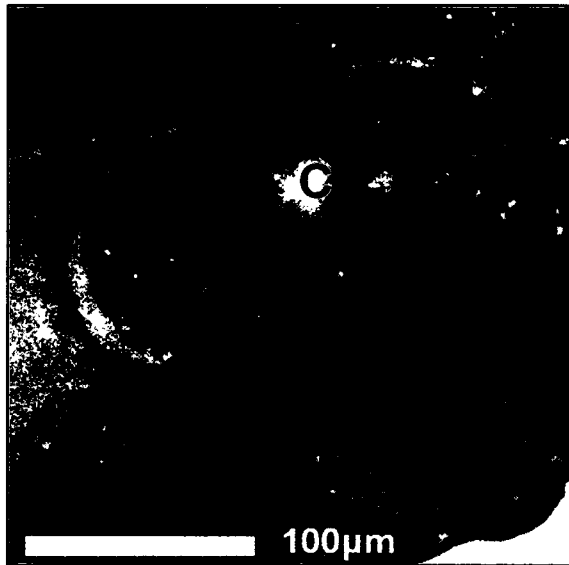


Figure 5: SEM-CL image of the core region of a polished otolith. Daily increments are visible occurring in concentric bands surrounding a luminescent central core region (C).

Figure 6.

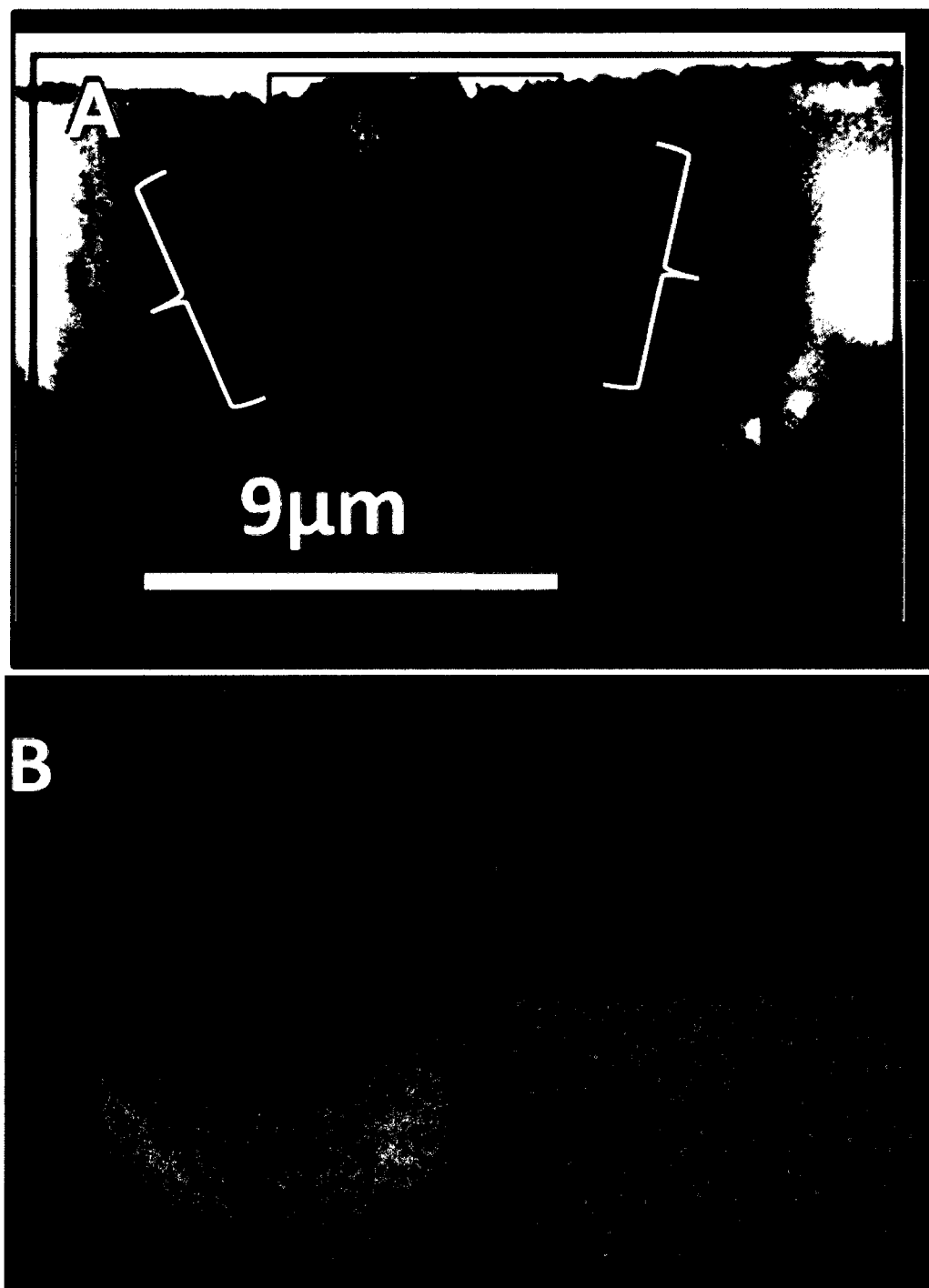


Figure 6: (A) SEM-BSE image of primordia cluster (purple box) and the core boundary (light-coloured band highlighted by white brackets). (B) SEM-EDS maps of C (red), O (orange), Ca (yellow) and Mn (blue) collected from sample surface shown in Figure 6A.

Figure 7.

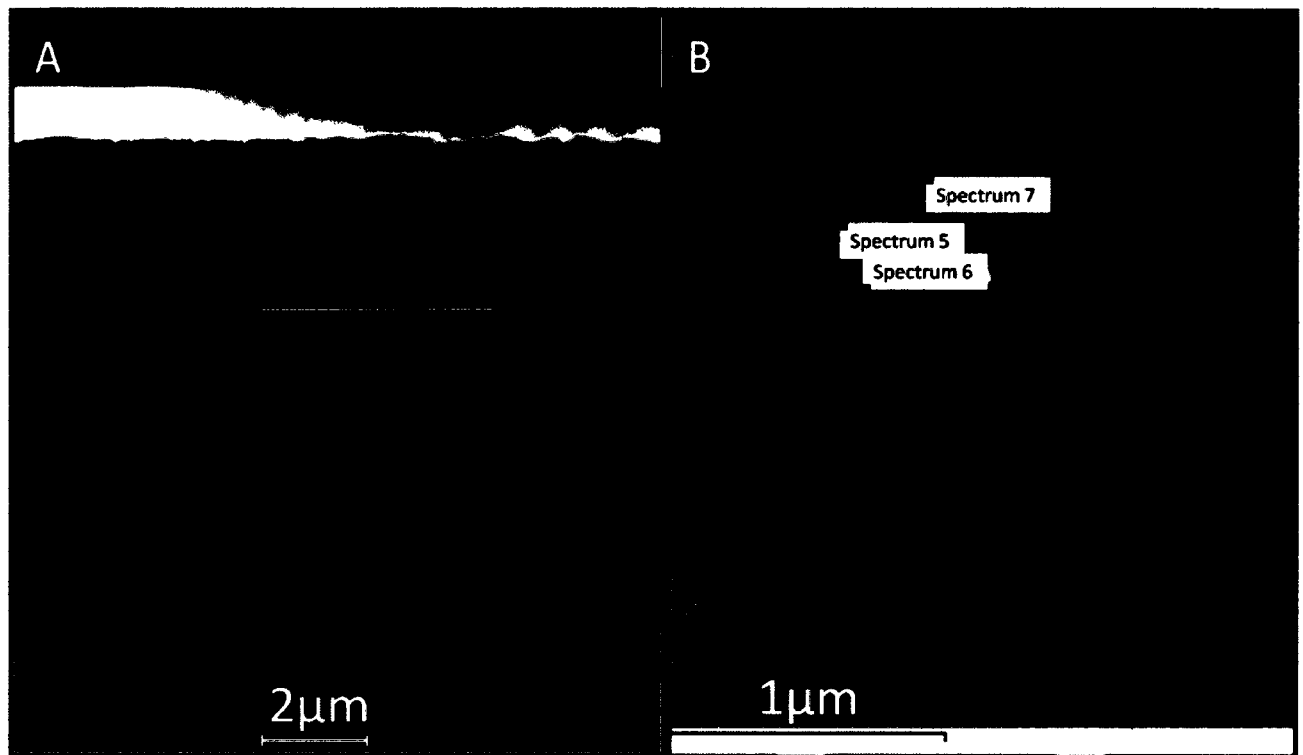


Figure 7: (A) TEM-HAADF image of the thin section milled from a region of the post-hatch otolith. Lighter, round nodules appear across sample surface area. Protective Pt coating on thin section appears as a bright layer along the top of the sample. (B) TEM-HAADF image of nodule; locations where EDS spectra were collected are labeled and denoted by small purple squares. EDS data included in Table 1.

Figure 8.

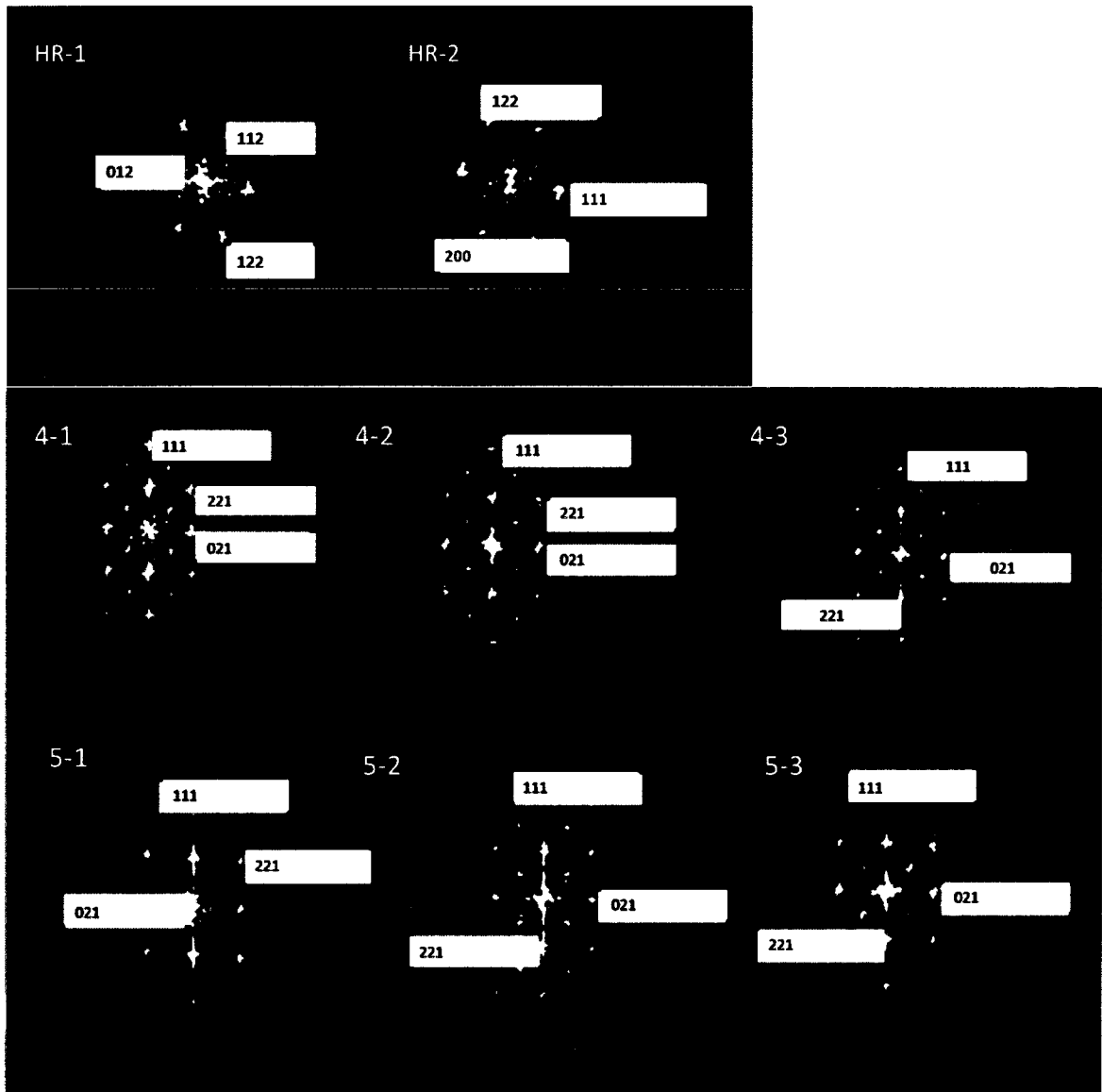


Figure 8: Accompanying FFT of locations denoted in Table 2 (d-spacings inset).

Figure 9.

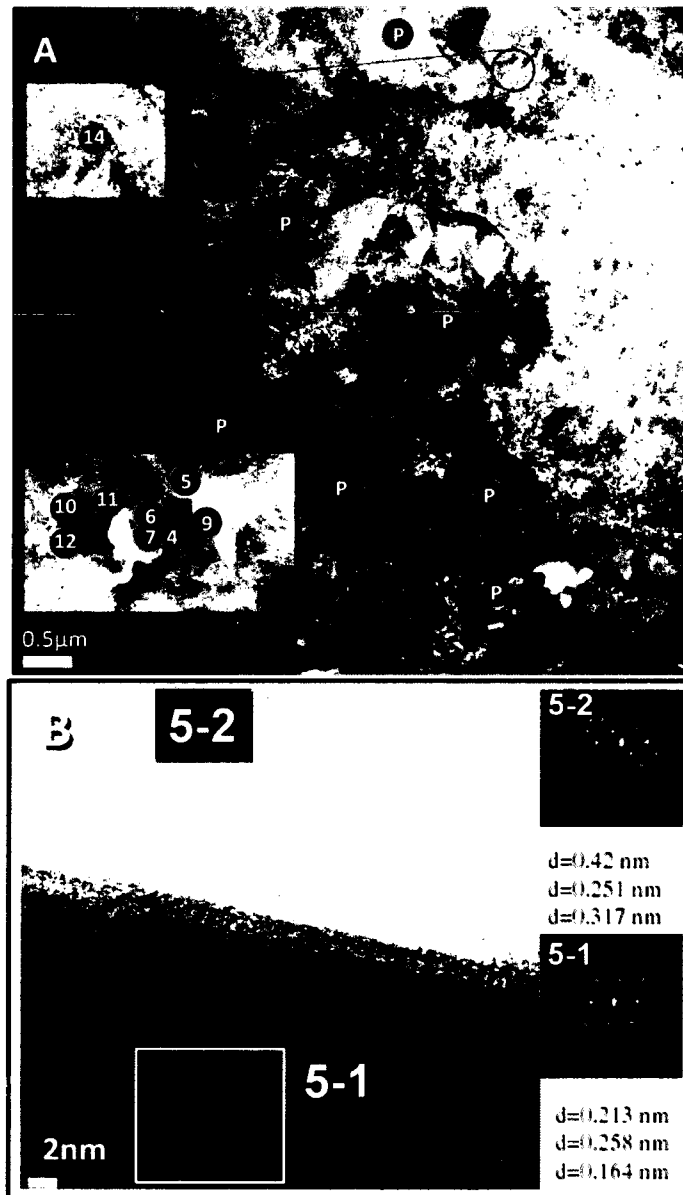


Figure 9: (A) TEM-BF image of the thin section milled to include the otolith core region. Multiple circular primordia (denoted by "P") appear throughout. Numbers denote regions where high resolution images (and in some cases, FFT of these images) were collected (B) Bright field image of the interface between a primordium and the rest of the otolith core; an amorphous border separates the darker primordium interior and lighter exterior core region. Region 5-1 and 5-2 denote two areas where FFT (inset, right) was conducted on HRTEM images and d-spacings are included that were calculated from images of each area.

Figure 10.

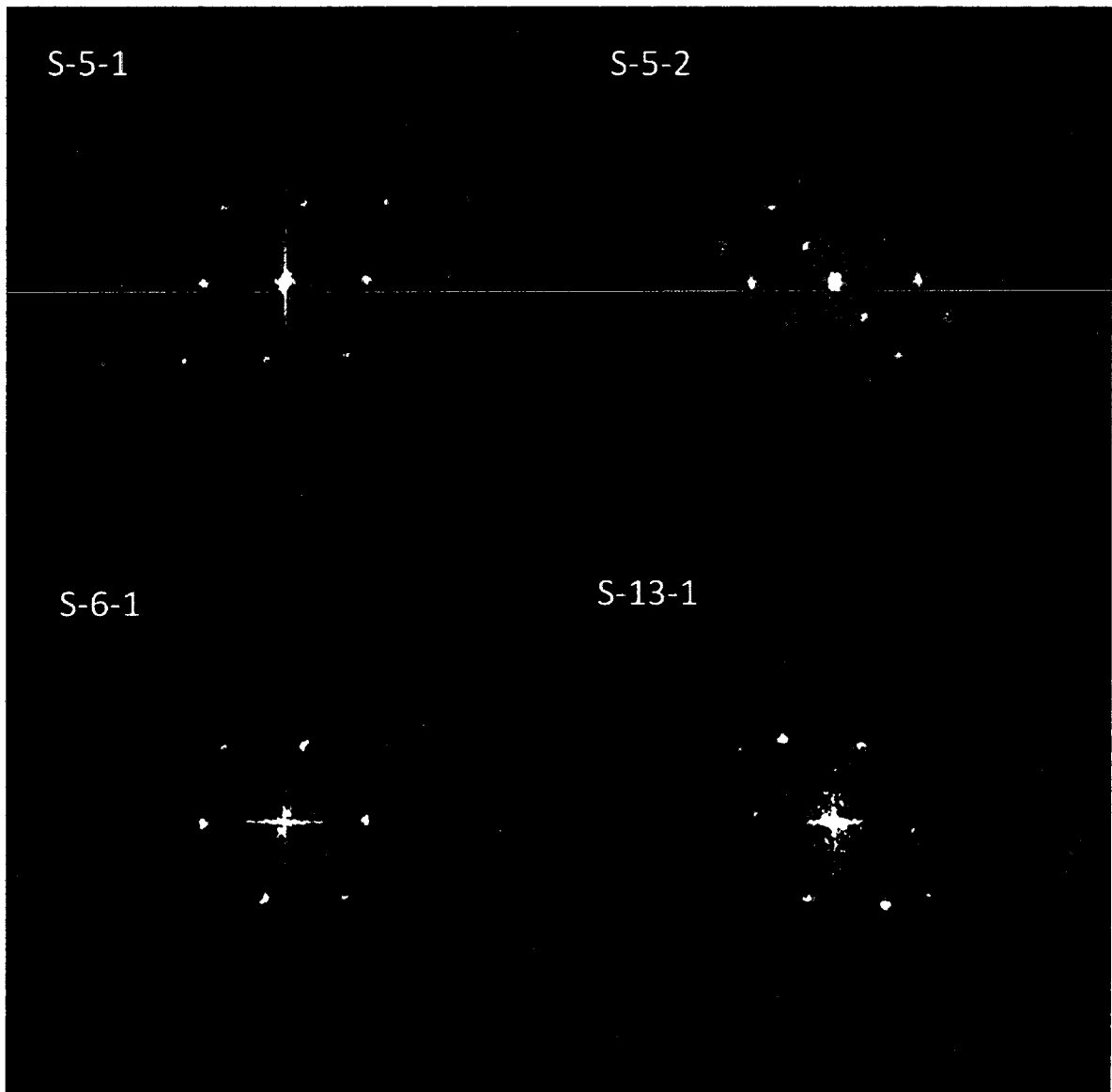


Figure 10: FFT images accompanying locations denoted in Table 3. S-5-1 and S-5-2 are also observed inset in Figure 9B.

Figure 11.

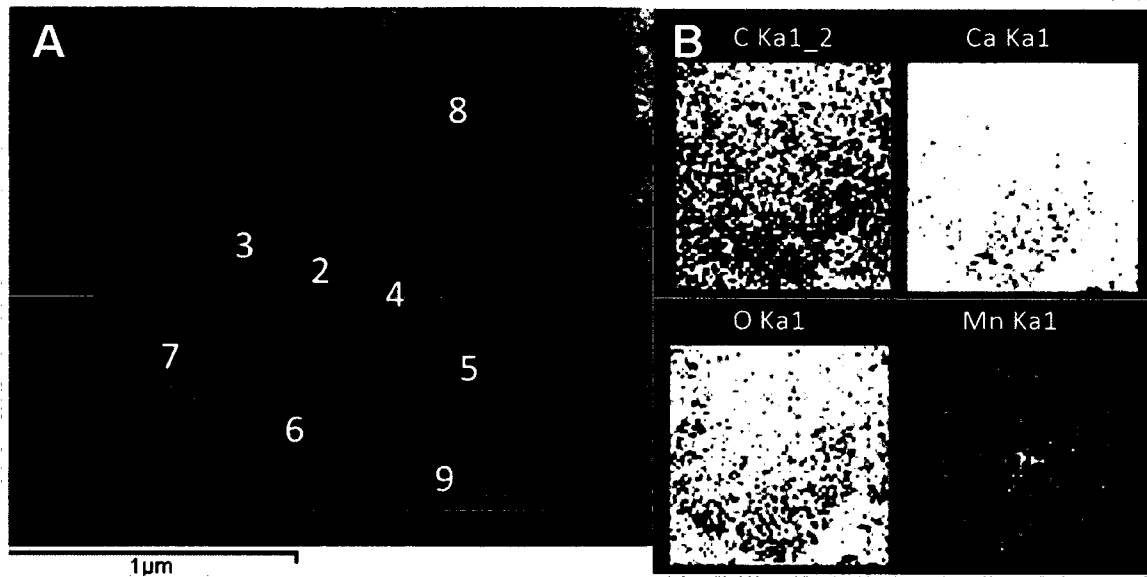


Figure 11: (A) TEM-HAADF image of a single primordium (large boxed region) in the thin section milled to include the otolith core region. Numbered boxed regions denote areas where EDS spectra were collected (spectra values included in Table 4). (B) STEM element maps of C, Ca, O and Mn. C, Ca and O appear to be less concentrated in the primordium. Mn occurs in relatively high concentrations at the centre of the primordium, and at the interface between the primordium and the surrounding core region.

VITA AUCTORIS

Desirée Chevalier was born in Windsor, Ontario, Canada in 1984. She graduated from Essex District High School (Essex, ON) in 2003. She went to the University of Windsor and graduated with a B.A.S in 2008, majoring in Earth Sciences and History with a minor in Biology. She is currently a candidate for a Master's degree in Science from the Great Lakes Institute for Environmental Research at the University of Windsor and plans to graduate in October 2010.